MiR-16-5p is frequently down-regulated in astrocytic gliomas and modulates glioma cell proliferation, apoptosis, and response to cytotoxic therapy

Krell, Anneliese ; Wolter, Marietta ; Stojcheva, Nina ; Hertler, Caroline ; Liesenberg, Franziska ; Zapatka, Marc ; Weller, Michael ; Malzkorn, Bastian ; Reifenberger, Guido

Abstract: AIMS Aberrant expression of microRNAs (miRNAs) is frequent in various cancers including gliomas. We aimed to characterize the role of miR-16-5p as a candidate tumour suppressor miRNA in gliomas. METHODS Real-time PCR-based approaches were used for miRNA and mRNA expression profiling of glioma and non-neoplastic brain tissues as well as glioma cell lines. Protein levels were determined by Western blotting. In vitro analyses were performed following overexpression of miR-16-5p, trichostatin A treatment, and siRNA-mediated knock-down of HDAC3 in glioma cells. Effects of miR-16-5p on glioma cell viability, apoptosis and response to irradiation and temozolomide were assessed. RESULTS Expression of miR-16-5p was reduced relative to control brain tissue in isocitrate dehydrogenase (IDH)-mutant astrocytomas of World Health Organization (WHO) grades II, III, and IV, and a subset of IDH-wildtype glioblastomas WHO grade IV. MiR-16-5p expression was lower in IDH-mutant than in IDH-wildtype gliomas, and down-regulated in IDH-wildtype glioma lines. MiR-16-5p overexpression reduced expression of important cell cycle and apoptosis regulators in glioma cells, including CDK6, CDC25A, CCND3, CCNE1, WEE1, CHEK1, BCL2, and MCL1. In line, CDK6, WEE1, CHEK1, BCL2, and MCL1 transcript levels were increased in WHO grade III or IV gliomas. Trichostatin A treatment and HDAC3 knockdown in glioma cells induced miR-16-5p up-regulation and reduced expression of its targets. Moreover, miR-16-5p overexpression inhibited proliferation and induced apoptosis in various glioma cell lines and increased sensitivity of A172 glioma cells to irradiation and temozolomide. CONCLUSION Reduced expression of miR-16-5p contributes to glioma cell proliferation, survival, and resistance to cytotoxic therapy. This article is protected by copyright. All rights reserved.

DOI: https://doi.org/10.1111/nan.12532

Neuropathology and Applied Neurobiology

BNS

MiR-16-5p is frequently down-regulated in astrocytic gliomas and modulates glioma cell proliferation, apoptosis, and response to cytotoxic therapy

Journal:	*Neuropathology and Applied Neurobiology*
Manuscript ID	NAN-2018-0231.R1
Manuscript Type:	Original Article
Date Submitted by the Author:	29-Nov-2018
Complete List of Authors:	Krell, Anneliese; Universitatsklinikum Dusseldorf, Neuropathologie Wolter, Marietta; Universitatsklinikum Dusseldorf, Neuropathologie Stojcheva, Nina; UniversitatsSpital Zurich, Neurologie Hertler, Caroline; UniversitatsSpital Zurich, Neurologie Liesenberg, Franziska; Universitatsklinikum Dusseldorf, Neuropathologie Zapatka, Marc; Deutsches Krebsforschungszentrum, Abteilung für Molekulare Genetik Weller, Michael; UniversitatsSpital Zurich, Neurologie Malzkorn, Bastian; Universitatsklinikum Dusseldorf, Neuropathologie Reifenberger, Guido; Heinrich-Heine-University, ;
Keywords:	apoptosis, glioma, miR-16-5p, proliferation, temozolomide resistance

MiR-16-5p is frequently down-regulated in astrocytic gliomas and modulates glioma cell proliferation, apoptosis, and response to cytotoxic therapy

Anneliese Krell,[1#] Marietta Wolter,[1#] Nina Stojcheva,[2] Caroline Hertler,[2] Franziska Liesenberg,[1] Marc Zapatka,[3] Michael Weller,[2] Bastian Malzkorn,[1*] Guido Reifenberger[1,4*]

[1]Department of Neuropathology, Heinrich Heine University, Düsseldorf, Germany; [2]Department of Neurology, University Hospital Zurich, Zurich, Switzerland; [3]Division of Molecular Genetics, German Cancer Research Center, Heidelberg, Germany; [4]German Cancer Consortium (DKTK), partner site Essen/Düsseldorf, DKFZ, Heidelberg, Germany

[#] These authors share first authorship

* These authors share senior authorship

Corresponding author: Guido Reifenberger, Department of Neuropathology, Heinrich Heine University, Moorenstrasse 5, D-40225 Düsseldorf, Germany, Phone: +49 211 8118660, Fax: +49 211 8117804, E-mail: reifenberger@uni-duesseldorf.de

Key words: apoptosis, glioma, *miR-16-5p*, proliferation, temozolomide resistance

Short title: *miR-16-5p* in astrocytic gliomas

Text word count: 4967 words

Number of figures: 7 (plus 3 Supplementary Figures)

Number of tables: 1 Supplementary Table

Abstract

Aims: Aberrant expression of microRNAs (miRNAs) is frequent in various cancers including gliomas. We aimed to characterize the role of *miR-16-5p* as a candidate tumour suppressor miRNA in gliomas.

Methods: Real-time PCR-based approaches were used for miRNA and mRNA expression profiling of glioma and non-neoplastic brain tissues as well as glioma cell lines. Protein levels were determined by Western blotting. *In vitro* analyses were performed following overexpression of *miR-16-5p*, trichostatin A treatment, and siRNA-mediated knock-down of *HDAC3* in glioma cells. Effects of *miR-16-5p* on glioma cell viability, apoptosis and response to irradiation and temozolomide were assessed.

Results: Expression of *miR-16-5p* was reduced relative to control brain tissue in isocitrate dehydrogenase (IDH)-mutant astrocytomas of World Health Organization (WHO) grades II, III, and IV, and a subset of IDH-wildtype glioblastomas WHO grade IV. *MiR-16-5p* expression was lower in IDH-mutant than in IDH-wildtype gliomas, and down-regulated in IDH-wildtype glioma lines. *MiR-16-5p* overexpression reduced expression of important cell cycle and apoptosis regulators in glioma cells, including CDK6, CDC25A, CCND3, CCNE1, WEE1, CHEK1, BCL2, and MCL1. In line, *CDK6*, *WEE1*, *CHEK1, BCL2,* and *MCL1* transcript levels were increased in WHO grade III or IV gliomas. Trichostatin A treatment and *HDAC3* knockdown in glioma cells induced *miR-16-5p* up-regulation and reduced expression of its targets. Moreover, *miR-16-5p* overexpression inhibited proliferation and induced apoptosis in various glioma cell lines and increased sensitivity of A172 glioma cells to irradiation and temozolomide.

Conclusion: Reduced expression of m*iR-16-5p* contributes to glioma cell proliferation, survival, and resistance to cytotoxic therapy.

Abstract word count: 248 words

Abbreviations used: CLL, chronic lymphocytic leukaemia; IDH, isocitrate dehydrogenase; miRNA, micro-RNA; pre-miR-16-5p, synthetic miR-16-5p precursor molecules; pre-miR-NC, synthetic negative control miRNA precursor molecules; TCGA, The Cancer Genome Atlas; TMZ, temozolomide; TSA, trichostatin A; 3'-UTR, 3'-untranslated region**;** WHO, World Health Organization

Introduction

Gliomas are the most common intrinsic brain tumours and comprise a spectrum of neoplastic lesions with distinct molecular and histological features, biological behaviour, and clinical outcome. The prognosis of glioma patients depends on tumour type and grade according to the World Health Organization (WHO) classification of tumours of the central nervous system (1), as well as on clinical parameters such as patient age, clinical performance status, and extent of tumour resection (2). In addition, molecular biomarkers have been identified that are linked to prognosis and/or response to cytotoxic therapy, such as mutations in the isocitrate dehydrogenase (IDH) genes *IDH1* or *IDH2*, co-deletion of chromosomal arms 1p and 19q, and O^6-methylguanine DNA-methyltransferase (*MGMT*) promoter methylation (3), with IDH mutation and 1p/19q codeletion serving as novel diagnostic molecular biomarkers in the WHO classification 2016 (1). IDH-wildtype glioblastoma is the most common and most malignant glioma entity that requires up-front multimodal therapy consisting in surgical resection followed by radiotherapy with concomitant and maintenance temozolomide (TMZ) as the current standard of care (2, 4). Despite this aggressive treatment, glioblastomas invariably relapse and become resistant to radio- and chemotherapy. This in turn limits the prognosis to median overall survival times of approximately 16 months in clinical trials and less than 12 months in population-based studies (2). Therefore, it is of paramount importance to better understand the molecular mechanisms driving glioma growth and underlying radio- and chemotherapy resistance in order to develop more effective therapeutic strategies.

Here, we addressed the role of a specific microRNA (miRNA), *miR-16-5p*, in glioma pathogenesis and therapy resistance. MiRNAs are small, non-coding RNAs that regulate gene expression preferentially by binding to the 3´-untranslated region (3'-UTR) of mRNAs in a sequence specific manner, thereby leading to inhibition of translation and/or enhanced mRNA degradation (5, 6). Altered miRNA expression, including down-regulation of tumour

suppressive and up-regulation of tumour promoting miRNAs, have been identified in many cancers (6), including gliomas (7–9). Among the first miRNAs implicated as tumour suppressors was *miR-16-5p,* which belongs to a family of evolutionary conserved miRNAs that share a common seed sequence. *MiR-16-5p* is transcribed from two miRNA clusters on different chromosomes (10, 11). The *miR-15b-16-2* cluster is located on chromosome 3 intronic to the *SMC4* gene, while the *miR-15a-16-1* cluster is located on chromosome 13 intronic to the *DLEU2* gene (12, 13). The latter cluster is frequently affected by deletions in chronic lymphocytic leukaemia (CLL) (14).

Using stem-loop reverse transcription PCR-based expression profiling of 79 astrocytic gliomas, we identified reduced levels of *miR-16-5p* expression in IDH-mutant astrocytic gliomas and a subset of IDH-wildtype glioblastomas relative to non-neoplastic brain tissue. Subsequent molecular and functional analyses provided further support for a role of *miR-16-5p* in regulating glioma cell proliferation and apoptosis, as well as modulating response of glioma cells to cytotoxic therapy.

Materials and methods

Human glioma tissue samples

Deep-frozen glioma tissue samples were retrieved from the tumour tissue bank at the Department of Neuropathology, Heinrich Heine University, Düsseldorf, Germany, and investigated as approved by the institutional review board (study number 3904). All tumours were classified according to the WHO classification of tumours of the central nervous system (1). Tissue samples used for nucleic acid extraction were histologically evaluated to assure an estimated tumour cell content of 80 % or more. We investigated tumour tissue samples from 79 patients, including seven patients with diffuse astrocytomas, IDH-mutant (WHO grade II), 10 patients with anaplastic astrocytomas, IDH-mutant (WHO grade III), 10 patients

with glioblastomas, IDH-mutant (WHO grade IV), and 52 patients with glioblastomas, IDH-wildtype (WHO grade IV). Ten commercially available RNA samples from non-neoplastic human brain tissues (Ambion, Austin, TX; BioChain, Hayward, CA; Clontech, Mountain View, CA; Stratagene, Cedar Creek, TX) were used as normal tissue reference samples. The IDH mutation status of each tumour was determined by sequencing of the regions encoding IDH1 codon 132 and IDH2 codon 172 (15, 16).

Glioma cell lines

A172, T98G, U251MG, U138MG, and U87MG cells were purchased from American Type Culture Collection (Manassas, VA, USA). TP365MG cells were provided by Dr. V. P. Collins (Cambridge, UK). Genotyping was performed at the Leibniz Institute DSMZ – German Collection of Microorganisms and Cell Cultures (Braunschweig, Germany) for authentication of each cell line. Glioma cells were grown as monolayer cultures in Dulbecco´s modified Eagle´s medium (Life Technologies, Darmstadt, Germany) supplemented with 10 % heat-inactivated fetal calf serum and 1 % penicillin G/streptomycin at 37°C and 5 % CO_2 in a humidified incubator. RNA was extracted from cultured glioma cells using the TRIzol reagent (Life Technologies).

Real-time reverse transcription PCR analyses

Expression profiling of 79 astrocytic gliomas and 9 non-neoplastic brain samples for differential expression of 365 miRNAs was performed on an ABI PRISM 7900HT system using TaqMan® Array MicroRNA cards with dye-labelled TaqMan® probes to monitor amplification (Life Technologies, Foster City, CA). Fluorescent data were converted into cycle threshold measurements by the SDS system software and exported to Microsoft Excel.

Four miRNAs (*miR-30a-5p*, *miR-30b*, *miR-30c*, *miR-30d*) with stable expression across the data set were used as reference for data normalization by SLqPCR (17).

Targeted expression analyses of *miR-16-5p* in glioma cell lines were performed on a StepOnePlus™ Real-Time PCR system (Life Technologies) using the miRCURY LNA™ Universal RT microRNA PCR kit and LNA™-enhanced PCR primers (Exiqon, Vedbaek, Denmark, *miR-16-5p* #205702). Fold expression changes relative to a calibrator sample (Universal Human Reference RNA, Stratagene, Cedar Creek, TX) were calculated with the $2^{-\Delta\Delta Ct}$ method (18) using *U6 snRNA* (Exiqon, #203907) as reference. Expression of *miR-16-5p* target genes was determined by real-time reverse transcription-PCR using SYBR Green® (Life Technologies) incorporation and the StepOnePlus™ system with *ARF1* (ADP-ribosylation factor 1) as reference transcript. Each real-time PCR experiment was performed in technical duplicates. For primer sequences see Supplementary Table 1.

Microarray-based mRNA expression analyses

Data on mRNA expression analyses of the *miR-16-5p* targets *CDK6, CDC25A, CCND3, CCNE1, WEE1, CHEK1, BCL2,* and *MCL1* were retrieved from our published microarray data set obtained on 68 gliomas, including eight IDH-mutant diffuse astrocytomas, 10 IDH-mutant anaplastic astrocytomas, 11 IDH-mutant glioblastomas, 39 IDH-wildtype glioblastomas, and four non-neoplastic brain tissue samples (16).

Transient transfection of glioma cells

A172, T98G, and TP365MG glioma cell lines were transiently transfected with 25 or 50 nM precursor-miR-16-5p molecules (pre-miR-16-5p, Ambion®, Life Technologies, #PM10339) for 18 hours using Lipofectamine™ 2000 reagent (Life Technologies). To control for unspecific

effects of transfection and to monitor transfection efficacy, glioma cells were transiently transfected with scrambled control oligonucleotides, i.e., Cy3-labelled precursor miR™ negative control (pre-miR-NC) (Ambion®, Life Technologies #AM17120). Overexpression of *miR-16-5p* in pre-miR-16-5p-transfected versus pre-miR-NC-transfected cells was determined by real time-reverse transcription PCR.

Western blot analyses

Glioma cells were transiently transfected with 50 nM of pre-miR-16-5p or pre-miR-NC 24 hours after seeding in 6-well culture plates, followed by protein extraction 72 hours post transfection. Cells were washed twice in ice-cold phosphate-buffered saline (PBS) buffer and lysed in RIPA buffer (1 x phosphate-buffered saline (PBS), 1 % Triton X-100, 0.5 % sodium deoxycholate, 0.1 % sodium dodecylsulfate) supplemented with one tablet of Complete Protease Inhibitor Cocktail Tablets and PhosSTOP Phosphatase Inhibitor Cocktail Tablets (Roche, Mannheim, Germany) per 10 ml of RIPA buffer. Cell lysates were centrifuged and protein concentration in the supernatant was determined with the Pierce BCA protein assay kit (Thermo Scientific, Rockford, IL). Twenty-five micrograms of total protein were separated by SDS-PAGE, followed by blotting to PROTRAN® BA83 nitrocellulose membranes (Schleicher & Schuell BioScience, Dassel, Germany). Membranes were blocked with Odyssey® blocking buffer (LI-COR Biosciences, Lincoln, NE) followed by overnight incubation at 8°C with one of the following antibodies diluted in 1 x tris-buffered saline supplemented with 0.1 % Tween-20 (TBS-T): mouse anti-CDK6 (1:500; Cell Signaling, Danvers, MA; #3136), mouse anti-CCNE1 (1:500, Cell Signaling; #4129), mouse anti-CHEK1 (1:500, Cell Signaling; #2360), rabbit anti-BCL2 (1:500, Cell Signaling; #2870), rabbit anti-MCL1 (1:500, Cell Signaling; #4572), mouse anti-CDC25A (1:50, Santa Cruz Biotechnology, Dallas, TX; #sc-7389), mouse anti-WEE1 (1:50, Santa Cruz Biotechnology; #sc-5285), or mouse anti-CCND3 (1:50, Dako, Glosttrup, DK; #M7156). A rabbit anti-ACTB antibody (1:1000, Abcam, Cambridge, MA; #ab8227) was used to detect expression of beta-actin as house-keeping

control. Western blots were washed in 1 x TBS-T followed by incubation with the appropriate secondary antibodies: IRDye 680RD goat anti-mouse IgG (1:10000, LI-COR; #926-68070), IRDye 800CW goat anti-rabbit IgG (1:10000, LI-COR; #926-32211), IRDye 800CW goat anti-mouse IgG (1:10000, LI-COR; #926-32350), or IRDye 680RD goat anti-rabbit IgG (1:10000, LI-COR; #926-68071). Protein detection and quantification were performed using the Odyssey® Clx system (LI-COR). Each experiment was performed in triplicate.

Selection of predicted miRNA targets

Computational target prediction algorithms provided in Pictar (http://pictar.mdc-berlin.de/), and Targetscan 4.0 (http://www.targetscan.org) were used to select candidate targets of *miR-16-5p*. We specifically focused on targets involved in cell cycle and apoptosis regulation.

3´-UTR luciferase reporter gene assays

Parts of the 3´-untranslated regions (3'-UTRs) of *WEE1*, *CHEK1,* and *MCL1* encompassing the predicted *miR-16-5p* binding sites were amplified by PCR from genomic DNA. Parts of the 3´-UTR of *WEE1* or *MCL1* carrying mutated *miR-16-5p* binding sites were synthesized by Eurofins Genomics (Ebersberg, Germany). Parts of the *CHEK1* 3´-UTR with mutated binding sites were generated by overlap extension PCR. Wildtype or mutant sequences were cloned between the *XhoI* and *NotI* restriction sites downstream of the *Renilla* luciferase coding sequence in the psiCHECK™-2 vector (Promega, Mannheim, Germany). The psiCHECK™-2 vector also contains the *Firefly* luciferase gene whose robust expression from a Herpes simplex virus tyrosine kinase (HSV-TK) promoter allows for normalization of *Renilla* luciferase expression. Each construct was verified by DNA sequencing. For luciferase reporter gene assays, T98G cells were cultured in 96-well plates and co-transfected with 100 ng of psiCHECK™-2 vector, either containing the wildtype or the mutated miRNA binding

sites, and 50 nM of pre-miR-16-5p or pre-miR-NC using Lipofectamine™ 2000 reagent (Life Technologies). Forty-eight or 72 hours after transfection, *Firefly* and *Renilla* luciferase activities were measured using the Dual-Glo® Luciferase Assay System (Promega). Experiments consisted of five technical replicates and each transfection was repeated twice. For primer sequences see Supplementary Table 1.

Treatment of glioma cells with trichostatin A

To screen for histone acetylation-dependent regulation of *miR-16-5p* expression, A172, T98G, TP365MG, and U138MG glioma cells were incubated 24 hours after seeding in medium containing 1 μM trichostatin A (TSA, Merck, Darmstadt, Germany) for 36 hours. Total RNA was then isolated from treated and untreated (control) cells using TRIzol® reagent (Life Technologies), followed by real time RT-PCR analysis for *miR-16-5p* expression.

SiRNA-mediated knock-down of HDAC3 in glioma cells

T98G, U87MG or U251MG glioma cells were transiently transfected with 50 nM siRNA against *HDAC3* (Qiagen; #SI00057316 and #SI00057337) using Lipofectamine™ 2000 reagent (Life Technologies). As control, cells were transiently transfected with Cy3-labelled negative control oligonucleotides (AllStars Negative siRNA Cy3, Qiagen; #1027281). Knock-down of *HDAC3* was verified by real time-reverse transcription PCR and Western blotting. All transfections were performed in three independent experiments.

Analysis of viability, proliferation and caspase-3/7 activity in glioma cells

The viability of A172, T98G, and TP365MG glioma cells transfected with pre-miR-16-5p molecules compared to pre-miR-NC-transfected cells was determined 72 hours post transfection using the CellTiter-Glo® Luminescent Cell Viability Assay (Promega, Mannheim, Germany). To analyse the effect of pre-miR-16-5p transfection on proliferation, the BrdU-based cell proliferation chemiluminescent ELISA test (Roche Diagnostics, Mannheim, Germany) was used. Cells were harvested 72 hours post transfection and the BrdU labelling solution was added 12 hours before harvesting. Caspase-3/7 activity in pre-miR-16-5p transfected cells was determined 72 hours post transfection using the luminescence-based Caspase-Glo® 3/7 Assay System (Promega). A Beckman Coulter PARADIGM™ detection platform was used for measurement of luminescence or fluorescence signals. Each experimental group consisted of five replicates. Each assay was repeated twice.

Determination of cell survival following irradiation or TMZ treatment

The effect of *miR-16-5p* on response of glioma cells to irradiation or TMZ was investigated as reported (19). Briefly, T98G or A172 glioma cells were seeded at 300 cells per well in 96-well plates in triplicates, allowed to adhere overnight, and exposed to TMZ at defined concentrations, according to respective EC50 values of each cell line (20), for 24 hours in serum-free medium, followed by an observation period for 2-3 weeks in serum-containing medium until untreated control cells reached confluence. Cell density was assessed by crystal violet staining. TMZ (Schering-Plough, Kenilworth, NJ, USA) was prepared as a stock solution at 100 mM in dimethyl sulfoxide (DMSO, Sigma, St. Louis, MO). For irradiation experiments, cells were irradiated in a 60-Co-radiation source (Gebrüder Sulzer, Thermische Energiesysteme, Winterthur, Switzerland) at defined doses in the range of 1 Gy – 9 Gy. The fraction of surviving cells following treatment was calculated in % relative to control cells.

Association of miR-16-5p expression with molecular markers and overall survival

Associations of *miR-16-5p* expression with IDH status and *TP53* mutation, as well as overall survival of glioma patients were investigated by using The Cancer Genome Atlas (TCGA) datasets (http://cancergenome.nih.gov/). Expression data were downloaded directly from the GDC data portal (https://portal.gdc.cancer.gov/) and via the cBio Cancer Genomics Portal (www.cbioportal.org) (21, 22) using the open-source R package "cgsdr" (version 1.2.5) and the statistical computing language R (version 3.3.2). Published biomarker information on IDH status and 1p/19q codeletion status (23) was used to classify tumours according to the WHO classification (1). To investigate the association of *miR-16-5p* expression with patient survival, we divided the TCGA cohorts into patients with tumours showing low or high expression using the median level as cut-off. Survival data were obtained from a previous TCGA paper (23). Kaplan-Meier survival probability estimates were calculated using the R-Package "Survival" (version 2.40-1).

Statistical analysis

Expression differences between glioma groups were analysed by two-sided Student´s t-test (two groups) or ANOVA and Dunnett's post-hoc test (multiple groups). Correlation of expression levels was analysed by calculating Pearson's r and a corresponding p-value (t-test). Differences in overall survival between patient groups with high and low miRNA expression were investigated by calculating Kaplan-Meier survival curves and use of a logrank-test. Statistical analysis of luminescence (viability, proliferation) or fluorescence (caspase-3/7 activity) values derived from pre-miR-16-5p-transfected versus pre-miR-NC-transfected cells of three independent experiments with five replicates per experimental group were analysed by a mixed model. Two-sided paired Student´s t-test was used to compare the mean luminescence values between pre-miR-16-5p- and pre-miR-NC-transfected glioma cells in the luciferase reporter gene assay. TSA-treated glioma cells

versus control cells and siRNA-transfected versus control-transfected cells were compared using two-sided paired Student´s t-test. Cell survival assay results of treated samples were normalized to the respective untreated control values. Significance was assessed using two-sided unpaired Student's t-test. Differences or associations were considered as significant with $p < 0.05$.

Results

Reduced expression of miR-16-5p in astrocytic gliomas and glioma cell lines relative to non-neoplastic brain tissue

We performed miRNAs expression profiling of primary tumour samples from 79 patients with astrocytic gliomas of WHO grades II, III or IV using TaqMan® Array microfluid cards. Thereby, we identified reduced mean expression levels of *miR-16-5p* relative to non-neoplastic brain tissue in IDH-mutant diffuse astrocytomas WHO grade II (AII^{mut}, 5.6-fold reduced mean *miR-16-5p* expression, $p<0.01$), IDH-mutant anaplastic astrocytomas of WHO grade III ($AAIII^{mut}$, 4.9-fold reduced mean *miR-16-5p* expression, $p<0.01$), and IDH-mutant glioblastomas of WHO grade IV ($GBIV^{mut}$, 3.1-fold reduced mean *miR-16-5p* expression, $p < 0.05$). In IDH-wildtype glioblastomas ($GBIV^{wt}$), expression of *miR-16-5p* was more heterogeneous. Although mean expression in this group was not significantly lower as compared to the non-neoplastic brain tissue samples, 34 of 52 investigated tumours showed reduced expression levels relative to the median *miR-16-5p* expression in the control samples (Fig. 1A). *MiR-16-5p* expression was significantly lower in 27 IDH-mutant as compared to 52 IDH-wildtype gliomas of our cohort (Fig. 1B). We also investigated six IDH-wildtype glioma cell lines (A172, T98G, U251MG, U138MG, U87MG, TP365MG) and found reduced *miR-16-5p* expression levels relative to non-neoplastic brain tissue samples (Fig. 1C).

Overexpression of miR-16-5p decreases glioma cell viability, reduces proliferation, and induces caspase-3/7 activity

To determine the functional roles of *miR-16-5p* in glioma cells, we transiently overexpressed precursor molecules of *miR-16-5p* (pre-miR-16-5p) or respective non-targeting control oligonucleotides (pre-miR-NC) in three glioma cell lines (A172, T98G, and TP365MG), followed by determination of cell viability (Fig. 2A), proliferation (Fig. 2B) and caspase-3/7 activity (Fig. 2C). Transfection of pre-miR-16-5p significantly decreased cell viability and proliferation in all three cell lines when compared to control-transfected cells. Caspase-3/7 activity was significantly increased by pre-miR-16-5p transfection in the p53-wildtype A172 and TP365MG cell lines but decreased in p53-mutant T98G cells.

Overexpression of miR-16-5p reduces expression of regulators of cell cycle progression and apoptosis in glioma cells

MicroRNA target prediction showed that *miR-16-5p* has binding sites in the 3´-UTR of several genes that are involved in cell cycle progression and apoptosis. Most of these *miR-16-5p* targets have been validated by 3'-UTR luciferase assays in previous studies, including CDK6, CCND3, and CCNE1 (24, 25), CDC25A (26), WEE1, CHEK1 (27, 28), and BCL2 (25, 29). To investigate whether these targets are regulated by *miR-16-5p* in glioma cells, we transiently transfected A172 glioma cells with pre-miR-16-5p or pre-miR-NC. Overexpression of *miR-16-5p* resulted in significantly reduced mRNA expression of *CDK6*, *CCND3*, *CCNE1*, *CDC25A*, *WEE1,* and *CHEK1* in A172 glioma cells (Fig. 3A). Levels of the respective proteins as well as BCL2 and MCL1 also were significantly reduced following *miR-16-5p* overexpression (Fig. 3B, C). Similar results were obtained in TP365MG and U251MG glioma cells (Suppl. Fig. 1).

MiR-16-5p directly binds to the 3´-UTRs of WEE1, CHEK1, and MCL1

To validate that *miR-16-5p* directly binds to the 3´-UTR of *WEE1*, *CHEK1*, and *MCL1*, we performed luciferase reporter assays using 3'-UTR fragments of each gene containing either the wildtype or mutated *miR-16-5p* binding sites. These experiments revealed specific binding of *miR-16-5p* to the 3'-UTR of all three genes (Fig. 4).

Expression of miR-16-5p target genes in astrocytic gliomas

To assess mRNA expression of the selected *miR-16-5p* target genes in glioma tissues, we referred to our published microarray data set (16), which showed that five of the eight investigated *miR-16-5p* targets (*CDK6*, *WEE1*, *CHEK1*, *BCL2*, and *MCL1*) showed significantly higher mRNA expression in anaplastic astrocytomas and/or glioblastomas when compared to non-neoplastic brain tissue (Fig. 5).

Trichostatin A increases miR-16-5p expression in glioma cells

Involvement of DNA methylation and histone modifications have been implicated in the regulation of *miR-16-5p* in CLL (30) and non-small cell lung cancer (31). Therefore, we investigated whether treatment of A172, T98G, TP365MG, and U138MG glioma cells with the histone deacetylase inhibitor TSA had an impact on *miR-16-5p* expression. These experiments revealed significant up-regulation of *miR-16-5p* following TSA treatment in three of the four investigated cell lines (Fig. 6A).

HDAC3 knock-down increases miR-16-5p expression in glioma cells

Previous studies in non-Hodgkin B-cell lymphomas and non-small cell lung cancers reported that MYC and HDAC3 co-localize to the promoters of the *miR-15a/miR-16-1* cluster host gene *DLEU2*, and that inhibition of HDAC3 increases histone acetylation of these promoters (31, 32). To investigate whether a similar mechanism operates in glioma cells, we performed

knock-down experiments of *HDAC3* in the glioma cell lines T98G and U251MG. Knock-down of *HDAC3* (Fig. 6B, C) significantly increased expression of *miR-16-5p* relative to control-transfected cells (Fig. 6D). We additionally investigated the expression of *miR-16-5p* target genes following *HDAC3* knock-down and found that most of the *miR-16-5p* target genes, including *CDK6*, *CCND3*, *CCNE1*, *CDC25A*, *WEE1,* and *CHEK1,* were significantly down-regulated following HDAC3 knock-down (Fig. 6 D, E), Supplementary Figure 3 shows the individual results obtained for expression of *miR-16-5p* and its target genes following *HDAC3* knock-down.

Overexpression of miR-16-5p modulates the response of A172 glioma cells to irradiation and chemotherapy

To assess whether overexpression of *miR-16-5p* modulates the response of glioma cells to irradiation or TMZ, we performed cell survival assays on pre-miR-16-5p- versus pre-miR-NC-transfected A172 and T98G glioma cells using radiation doses ranging from 1 to 9 Gy and TMZ concentrations ranging from 6.25 to 100 μM in A172 and 150 to 1000 μM in T98G cells (Fig. 7). A172 glioma cells are p53-wildtype glioma cells (33) that do not express O^6-methylguanine DNA methyltransferase (MGMT) due to hypermethylation of the *MGMT* promoter (34). In contrast, T98G glioma cells are p53-mutant (33) and express MGMT (35). As reported (34), A172 cells showed higher sensitivity to TMZ treatment than T98G cells (Fig. 7A, B). Sensitivity to TMZ was significantly increased in pre-miR-16-5p-transfected as compared to control-transfected A172 glioma cells (Fig. 7A). Similarly, pre-miR-16-5p-transfected A172 cells responded better to irradiation at clinically relevant radiation doses (Fig. 7C). In contrast, pre-miR-16-5p transfection did not modulate sensitivity of T98G cells to either TMZ treatment or irradiation (Fig. 7B, D).

Relationship of miR-16-5p expression with IDH and TP53 mutation status as well as overall survival in the TCGA cohort

To investigate the relationship of *miR-16-5p* expression with IDH and *TP53* mutation status as well as overall survival of glioblastoma patients, we interrogated TCGA data (http://cancergenome.nih.gov/). *MiR-16-5p* expression was lower in IDH-mutant than in IDH-wildtype gliomas (Supplementary Fig. 2A), thus confirming findings in our institutional cohort (Fig. 1B). As the expression of *miR-16-5p* may be regulated by p53 (36, 37), we also interrogated the TCGA database for a relationship between *TP53* mutation and *miR-16-5p* expression levels but found no association between these parameters (Suppl. Fig. 2B). *MiR-16-5p* expression was not linked to overall survival in 287 TCGA patients with glioblastomas, IDH-wildtype (WHO grade IV), when stratified according to high versus low expression levels (Suppl. Fig. 2C). Similarly, *miR-16-5p* expression was not prognostic in 214 TCGA patients with diffuse or anaplastic astrocytomas, IDH-mutant (WHO grades II or III) (Suppl. Fig. 2D).

Discussion

In this study we report that expression of *miR-16-5p* is reduced in IDH-mutant astrocytic gliomas as well as a subset of IDH-wildtype glioblastomas relative to non-neoplastic brain tissue. Moreover, *miR-16-5p* expression is down-regulated in IDH-wildtype glioblastoma cell lines. *MiR-16-5p* was discovered as a deleted and down-regulated tumour suppressor candidate in B-cell CLL (14). Since then, numerous studies reported on deletion and/or reduced expression of this miRNA in various types of tumours, ranging from pituitary adenoma (38) to carcinomas of the prostate (39), lung (40), pancreas (41), stomach (42), breast (43), and ovaries (44), as well as other cancers (45). Several studies have also addressed expression of *miR-16-5p* in gliomas, with partly conflicting results. We originally reported that *miR-16-5p* was up-regulated upon progression of primary low-grade to

recurrent high-grade gliomas from individual patients (46). However, expression of *miR-16-5p* was significantly lower in primary and recurrent glioma tissues as compared to non-neoplastic brain tissue, a finding in line with our present data on a larger patient cohort. In contrast, Wuchty *et al.* (47) reported higher expression levels of *miR-16-5p* in primary glioblastomas as compared to normal brain tissue. This discrepancy might in part be explained by the use of different reference tissues and our finding that down-regulation of *miR-16-5p* is more frequent and stronger in IDH-mutant as compared to IDH-wildtype gliomas. Nevertheless, other authors also found increased levels of *miR-16-5p*, but not of its host gene *DLEU2,* in glioblastomas and oligodendrogliomas (48). In contrast, studies on glioma cell lines support a tumour suppressive role of *miR-16-5p* by demonstrating inhibitory effects of this miRNA on glioma cell proliferation, migration, invasion and epithelial-to-mesenchymal transition, as well as stimulatory effects on apoptosis (49–53). Recent data additionally reported that *miR-16-5p* inhibits glioma stem cell clonogenicity and xenograft growth (25). In line, we found that *miR-16-5p* inhibited proliferation of three glioma cell lines (A172, TP365MG, T98G) and increased caspase-3/7 activity in two of these (A172, TP365MG). Studies on other cancers including CLL (29), oesophageal carcinoma (54), and non-small cell lung cancer (40), similarly reported on anti-proliferative and pro-apoptotic effects of *miR-16-5p*, thus establishing its tumour suppressive function.

To investigate mechanisms causing inhibition of glioma growth by *miR-16-5p*, we investigated eight cell cycle and/or apoptosis regulatory genes that carry binding sites for *miR-16-5p*, i.e., *CDK6, CCND3, CCNE1, CDC25A, WEE1, CHEK1, BCL2,* and *MCL1*. Following transient transfection of *miR-16-5p* precursor molecules into different glioma cell lines, we found reduced expression of each of these genes at the mRNA and/or protein levels. Previous studies had already shown that *miR-16-5p* directly binds the 3´-UTR of *CDK6*, *CCND3*, *CCNE1*, *CDC25A, and BCL2* (13, 24-26, 29, 39, 40, 51, 55, 56). Using 3´-UTR luciferase reporter assays we confirmed its specific binding to the 3'-UTR of *WEE1* and *CHEK1* (27, 28). Additional 3´-UTR luciferase reporter assays validated *MCL1* as a direct *miR-16-5p* target. Taken together, these data suggest that reduced expression of

miR-16-5p may promote glioma growth by facilitating up-regulation of positive regulators of cell cycle progression (CDK6, CCND3, CCNE1, CDC25A) and inhibitors of apoptosis (BCL2, MCL1). Moreover, *miR-16-5p* down-regulation in glioma cells caused increased expression of WEE1 and CHEK1, which may contribute to cell survival by preventing mitotic catastrophe as a consequence of massive replication stress (57–59).

MiR-16-5p overexpression may induce apoptosis by directly down-regulating BCL2 and MCL1 as originally reported in CLL (39, 60). In addition, overexpression of *miR-16-5p* activated the intrinsic apoptosis pathway via BCL2 in leukaemia cells (29). Former studies implicated BCL2 and MCL1 as important inhibitors of apoptosis also in glioma cells (61–65). Moreover, down-regulation of BCL2 and MCL1 by overexpression of another miRNA, *miR-153*, has been reported to induce apoptosis of glioma cells (66). Thus, several lines of evidence accumulate to support the hypothesis that reduced expression of *miR-16-5p* may promote glioma cell survival by preventing apoptosis through facilitating up-regulation of BCL2 and MCL1. At the same time, *miR-16-5p* down-regulation may facilitate glioma cell proliferation due to enhanced G1/S phase transition caused by up-regulation of e.g. CDK6 and CDC25A (25, 67, 68).

In line with the *in vitro* data, we found significantly increased mRNA expression levels of the *miR-16-5p* target genes *CDK6*, *WEE1, CHECK1, BCL2, and MCL1* in tissue samples of WHO grade III and/or WHO grade IV gliomas relative to non-neoplastic brain tissue, while no clear-cut up-regulation of CCNE1, CDC25A, and CCND3 was detected (16). Moreover, other studies reported on amplification and overexpression of *CDK6* (69, 70), increased expression of MCL1 and BCL2 (71), as well as up-regulation of WEE1 and CHEK1 expression in malignant gliomas (58, 72). Similarly, *CDC25A* mRNA expression has been reported to increase along with the proliferation rate of gliomas (68).

We also investigated potential mechanisms causing *miR-16-5p* down-regulation in gliomas. Studies on haematopoietic neoplasms showed that *miR-16-5p* expression may not only be reduced by copy number losses but also by epigenetic mechanisms, in particular histone

modifications (30–32). In B-cell lymphoma and lung carcinoma, transcription of *DLEU2* and the miR-*15a/miR-16-1* locus may be repressed by binding of MYC to *DLEU2* promoter regions, followed by recruitment of HDAC3 (31, 32). We provide evidence that a similar mechanism may be active in glioma. We observed that TSA treatment of glioma cells increased *miR-16-5p* expression, supporting a role of histone modifications in its transcriptional down-regulation. In addition, we showed that siRNA-mediated knock-down of *HDAC3* increased the expression of *miR-16-5p* with ensuing down-regulation of *miR-16-5p* target genes.

MiR-16-5p and p53 have been reported to interact in a feedback circuitry loop in CLL, in which p53 transactivates transcription of the miRNA, while the miRNA down-regulates p53 expression (27, 36, 60). Consequently, CLLs with *TP53* alterations showed decreased levels of *miR-16-5p* as well as elevated MCL1 expression (60). Using TCGA glioma datasets, however, we found no association between *TP53* mutation status and *miR-16-5p* expression, possibly due to the fact that astrocytic gliomas without *TP53* mutation typically carry alterations in other p53 pathway genes, such as *MDM2* or *MDM4* amplification, or $p14^{ARF}$ homozygous deletion (73).

MiR-16-5p directly regulates the expression of several genes that have been linked to therapy resistance like *BCL2, MCL1, WEE1, CHEK1,* and *CDK6* (58, 61, 74–77). In gliomas, *miR-16* has been reported to modulate TMZ resistance in U251MG glioma cells by regulating BCL2 (78). In addition, *miR-195*, a member of the *miR-15/miR-16* family, has been shown to inhibit glioma cell proliferation (79) and to modulate acquired resistance to TMZ (80). Moreover, members of the *miR-15/miR-16* family have been linked to resistance against other drugs, including cisplatin, doxorubicin and 5-fluorouracil (28, 81, 82). Therefore, we addressed potential effects of *miR-16-5p* overexpression on the response of glioma cells to irradiation and TMZ. We investigated A172 and T98G glioma cells transfected either with *miR-16-5p* precursors or non-targeting control oligonucleotides for sensitivity to irradiation or TMZ *in vitro*. The two cell lines represented a p53-wildtype, *MGMT* promoter-methylated

model (A172) and a p53-mutant, *MGMT* promoter-unmethylated model (T98G). We found that *miR-16-5p* increased sensitivity to irradiation and TMZ treatment in A172 but not in T98G cells, with the latter cells also being resistant to spontaneous caspase-3/7 induction upon overexpression of *miR-16-5p*. With respect to *miR-16-5p* as a therapeutic target, as it is under investigation in prostate carcinoma and pleural mesothelioma (83, 84), our findings suggest that response to *miR-16-5p* expression in glioma might depend on the genetic background of the tumour cells. This hypothesis, however, would require further experimental evaluation.

In TCGA data sets, we also addressed the question whether *miR-16-5p* expression is associated with overall survival of glioma patients. Expression of *miR-16-5p* was associated with overall survival in an institutional cohort of 132 glioblastoma patients (25). However, we found no prognostic role of high versus low *miR-16-5p* expression in 287 TCGA patients with IDH-wildtype glioblastoma and 214 TCGA patients with IDH-mutant diffuse or anaplastic astrocytomas. This discrepancy may be related to distinct patients cohorts, with the published cohort including younger patients (median age: 45 years) not specified for IDH status (25). In addition, different detection methods and *miR-16-5p* expression cut-offs were used.

In summary, we report on frequent down-regulation of *miR-16-5p* expression in astrocytic gliomas relative to non-neoplastic brain tissue, with expression levels being lower in IDH-mutant as compared to IDH-wildtype gliomas. Treatment with TSA or genetic silencing of *HDAC3* increased expression of *miR-16-5p* in glioma cells, suggesting a role of HDAC3-mediated histone modification in the transcriptional regulation of *miR-16-5p*, as reported for other cancers (31, 32, 85). Overexpression of *miR-16-5p* in glioma cells reduced expression of CDK6, CDC25A, CCND3, CCNE1, WEE1, CHEK1, BCL2, and MCL1, decreased cell proliferation and increased caspase-3/7 activity. In addition, *miR-16-5p* overexpression in A172 glioma cells increased sensitivity to irradiation and temozolomide treatment. Thus, *miR-16-5p* down-regulation may support glioma growth by facilitating higher expression of

various proteins that promote cell cycle progression and cell survival and may also contribute to resistance to cytotoxic treatment of these tumours.

References

1. Louis DN, Perry A, Reifenberger G, Deimling A von, Figarella-Branger D, Cavenee WK et al. The 2016 World Health Organization Classification of Tumours of the Central Nervous System: a summary. Acta Neuropathol 2016; 131(6):803–20.

2. Weller M, van den Bent M, Tonn JC, Stupp R, Preusser M, Cohen-Jonathan-Moyal E et al. European Association for Neuro-Oncology (EANO) guideline on the diagnosis and treatment of adult astrocytic and oligodendroglial gliomas. Lancet Oncol 2017; 18(6):e315-e329.

3. Reifenberger G, Wirsching H-G, Knobbe-Thomsen CB, Weller M. Advances in the molecular genetics of gliomas - implications for classification and therapy. Nat Rev Clin Oncol 2017; 14(7):434–52.

4. Stupp R, Mason WP, van den Bent, Martin J, Weller M, Fisher B, Taphoorn MJB et al. Radiotherapy plus concomitant and adjuvant temozolomide for glioblastoma. N Engl J Med 2005; 352(10):987–96.

5. Hayes J, Peruzzi PP, Lawler S. MicroRNAs in cancer: biomarkers, functions and therapy. Trends Mol Med 2014; 20(8):460–9.

6. Lin S, Gregory RI. MicroRNA biogenesis pathways in cancer. Nat Rev Cancer 2015; 15(6):321–33.

7. Ahir BK, Ozer H, Engelhard HH, Lakka SS. MicroRNAs in glioblastoma pathogenesis and therapy: A comprehensive review. Crit Rev Oncol Hematol 2017; 120:22–33.

8. Ames H, Halushka MK, Rodriguez FJ. miRNA Regulation in Gliomas: Usual Suspects in Glial Tumorigenesis and Evolving Clinical Applications. J Neuropathol Exp Neurol 2017; 76(4):246–54.

9. Banelli B, Forlani A, Allemanni G, Morabito A, Pistillo MP, Romani M. MicroRNA in Glioblastoma: An Overview. Int J Genomics 2017; 2017:7639084.

10. Finnerty JR, Wang W-X, Hébert SS, Wilfred BR, Mao G, Nelson PT. The miR-15/107 group of microRNA genes: evolutionary biology, cellular functions, and roles in human diseases. J Mol Biol 2010; 402(3):491–509.

11. Yue J, Tigyi G. Conservation of miR-15a/16-1 and miR-15b/16-2 clusters. Mamm Genome 2010; 21(1-2):88–94.

12. Garding A, Bhattacharya N, Claus R, Ruppel M, Tschuch C, Filarsky K et al. Epigenetic upregulation of lncRNAs at 13q14.3 in leukaemia is linked to the In Cis downregulation of a gene cluster that targets NF-kB. PLoS Genet 2013; 9(4):e1003373.

13. Lerner M, Harada M, Lovén J, Castro J, Davis Z, Oscier D et al. DLEU2, frequently deleted in malignancy, functions as a critical host gene of the cell cycle inhibitory microRNAs miR-15a and miR-16-1. Exp Cell Res 2009; 315(17):2941–52.

14. Calin GA, Dumitru CD, Shimizu M, Bichi R, Zupo S, Noch E et al. Frequent deletions and down-regulation of micro- RNA genes miR15 and miR16 at 13q14 in chronic lymphocytic leukaemia. Proc Natl Acad Sci U S A 2002; 99(24):15524–9.

15. Felsberg J, Wolter M, Seul H, Friedensdorf B, Göppert M, Sabel MC et al. Rapid and sensitive assessment of the IDH1 and IDH2 mutation status in cerebral gliomas based on DNA pyrosequencing. Acta Neuropathol 2010; 119(4):501–7.

16. Toedt G, Barbus S, Wolter M, Felsberg J, Tews B, Blond F et al. Molecular signatures classify astrocytic gliomas by IDH1 mutation status. Int J Cancer 2011; 128(5):1095–103.

17. Vandesompele J, Preter K de, Pattyn F, Poppe B, van Roy N, Paepe A de et al. Accurate normalization of real-time quantitative RT-PCR data by geometric averaging of multiple internal control genes. Genome Biol 2002; 3(7):RESEARCH0034.

18. Livak KJ, Schmittgen TD. Analysis of relative gene expression data using real-time quantitative PCR and the 2(-Delta Delta C(T)) Method. Methods 2001; 25(4):402–8.

19. Happold C, Roth P, Silginer M, Florea A-M, Lamszus K, Frei K et al. Interferon-β induces loss of spherogenicity and overcomes therapy resistance of glioblastoma stem cells. Mol Cancer Ther 2014; 13(4):948–61.

20. Hermisson M, Klumpp A, Wick W, Wischhusen J, Nagel G, Roos W et al. O6-methylguanine DNA methyltransferase and p53 status predict temozolomide sensitivity in human malignant glioma cells. J Neurochem 2006; 96(3):766–76.

21. Cerami E, Gao J, Dogrusoz U, Gross BE, Sumer SO, Aksoy BA et al. The cBio cancer genomics portal: an open platform for exploring multidimensional cancer genomics data. Cancer Discov 2012; 2(5):401–4.

22. Gao J, Ciriello G, Sander C, Schultz N. Collection, integration and analysis of cancer genomic profiles: from data to insight. Curr Opin Genet Dev 2014; 24:92–8.

23. Ceccarelli M, Barthel FP, Malta TM, Sabedot TS, Salama SR, Murray BA et al. Molecular Profiling Reveals Biologically Discrete Subsets and Pathways of Progression in Diffuse Glioma. Cell 2016; 164(3):550–63.

24. Liu Q, Fu H, Sun F, Zhang H, Tie Y, Zhu J et al. miR-16 family induces cell cycle arrest by regulating multiple cell cycle genes. Nucleic Acids Res 2008; 36(16):5391–404.

25. Tian R, Wang J, Yan H, Wu J, Xu Q, Zhan X et al. Differential expression of miR16 in glioblastoma and glioblastoma stem cells: their correlation with proliferation, differentiation, metastasis and prognosis. Oncogene 2017; 36(42):5861–73.

26. Pothof J, Verkaik NS, van IJcken W, Wiemer EAC, van Ta TB, van der Horst, Gijsbertus T J et al. MicroRNA-mediated gene silencing modulates the UV-induced DNA-damage response. EMBO J 2009; 28(14):2090–9.

27. Lezina L, Purmessur N, Antonov AV, Ivanova T, Karpova E, Krishan K et al. miR-16 and miR-26a target checkpoint kinases Wee1 and Chk1 in response to p53 activation by genotoxic stress. Cell Death Dis 2013; 4:e953.

28. Pouliot LM, Chen Y-C, Bai J, Guha R, Martin SE, Gottesman MM et al. Cisplatin sensitivity mediated by WEE1 and CHK1 is mediated by miR-155 and the miR-15 family. Cancer Res 2012; 72(22):5945–55.

29. Cimmino A, Calin GA, Fabbri M, Iorio MV, Ferracin M, Shimizu M et al. miR-15 and miR-16 induce apoptosis by targeting BCL2. Proc Natl Acad Sci U S A 2005; 102(39):13944–9.

30. Sampath D, Liu C, Vasan K, Sulda M, Puduvalli VK, Wierda WG et al. Histone deacetylases mediate the silencing of miR-15a, miR-16, and miR-29b in chronic lymphocytic leukaemia. Blood 2012; 119(5):1162–72.

31. Chen C-Q, Chen C-S, Chen J-J, Zhou L-P, Xu H-L, Jin W-W et al. Histone deacetylases inhibitor trichostatin A increases the expression of Dleu2/miR-15a/16-1 via HDAC3 in non-small cell lung cancer. Mol Cell Biochem 2013; 383(1-2):137–48.

32. Zhang X, Chen X, Lin J, Lwin T, Wright G, Moscinski LC et al. Myc represses miR-15a/miR-16-1 expression through recruitment of HDAC3 in mantle cell and other non-Hodgkin B-cell lymphomas. Oncogene 2012; 31(24):3002–8.

33. Ishii N, Maier D, Merlo A, Tada M, Sawamura Y, Diserens AC et al. Frequent co-alterations of TP53, p16/CDKN2A, p14ARF, PTEN tumour suppressor genes in human glioma cell lines. Brain Pathol 1999; 9(3):469–79.

34. Gaspar N, Marshall L, Perryman L, Bax DA, Little SE, Viana-Pereira M et al. MGMT-independent temozolomide resistance in pediatric glioblastoma cells associated with a PI3-kinase-mediated HOX/stem cell gene signature. Cancer Res 2010; 70(22):9243–52.

35. Wang X, Chen J-x, Liu Y-h, You C, Mao Q. Mutant TP53 enhances the resistance of glioblastoma cells to temozolomide by up-regulating O(6)-methylguanine DNA-methyltransferase. Neurol Sci 2013; 34(8):1421–8.

36. Fabbri M, Bottoni A, Shimizu M, Spizzo R, Nicoloso MS, Rossi S et al. Association of a microRNA/TP53 feedback circuitry with pathogenesis and outcome of B-cell chronic lymphocytic leukaemia. JAMA 2011; 305(1):59–67.

37. Shi L, Jackstadt R, Siemens H, Li H, Kirchner T, Hermeking H. p53-induced miR-15a/16-1 and AP4 form a double-negative feedback loop to regulate epithelial-mesenchymal transition and metastasis in colorectal cancer. Cancer Res 2014; 74(2):532–42.

38. Bottoni A, Piccin D, Tagliati F, Luchin A, Zatelli MC, Degli Uberti EC. miR-15a and miR-16-1 down-regulation in pituitary adenomas. J Cell Physiol 2005; 204(1):280–5.

39. Bonci D, Coppola V, Musumeci M, Addario A, Giuffrida R, Memeo L et al. The miR-15a-miR-16-1 cluster controls prostate cancer by targeting multiple oncogenic activities. Nat Med 2008; 14(11):1271–7.

40. Bandi N, Zbinden S, Gugger M, Arnold M, Kocher V, Hasan L et al. miR-15a and miR-16 are implicated in cell cycle regulation in a Rb-dependent manner and are frequently deleted or down-regulated in non-small cell lung cancer. Cancer Res 2009; 69(13):5553–9.

41. Jiao LR, Frampton AE, Jacob J, Pellegrino L, Krell J, Giamas G et al. MicroRNAs targeting oncogenes are down-regulated in pancreatic malignant transformation from benign tumours. PLoS ONE 2012; 7(2):e32068.

42. Kang W, Tong JHM, Lung RWM, Dong Y, Zhao J, Liang Q et al. Targeting of YAP1 by microRNA-15a and microRNA-16-1 exerts tumour suppressor function in gastric adenocarcinoma. Mol Cancer 2015; 14:52.

43. Rivas MA, Venturutti L, Huang Y-W, Schillaci R, Huang TH-M, Elizalde PV. Downregulation of the tumour-suppressor miR-16 via progestin-mediated oncogenic signaling contributes to breast cancer development. Breast Cancer Res 2012; 14(3):R77.

44. Bhattacharya R, Nicoloso M, Arvizo R, Wang E, Cortez A, Rossi S et al. MiR-15a and MiR-16 control Bmi-1 expression in ovarian cancer. Cancer Res 2009; 69(23):9090–5.

45. Aqeilan RI, Calin GA, Croce CM. miR-15a and miR-16-1 in cancer: discovery, function and future perspectives. Cell Death Differ 2010; 17(2):215–20.

46. Malzkorn B, Wolter M, Liesenberg F, Grzendowski M, Stühler K, Meyer HE et al. Identification and functional characterization of microRNAs involved in the malignant progression of gliomas. Brain Pathol 2010; 20(3):539–50.

47. Wuchty S, Arjona D, Li A, Kotliarov Y, Walling J, Ahn S et al. Prediction of Associations between microRNAs and Gene Expression in Glioma Biology. PLoS ONE 2011; 6(2):e14681.

48. Lages E, Guttin A, El Atifi M, Ramus C, Ipas H, Dupré I et al. MicroRNA and target protein patterns reveal physiopathological features of glioma subtypes. PLoS ONE 2011; 6(5):e20600.

49. Li X, Ling N, Bai Y, Dong W, Hui G-Z, Liu D et al. MiR-16-1 plays a role in reducing migration and invasion of glioma cells. Anat Rec (Hoboken) 2013; 296(3):427–32.

50. Wang Q, Li X, Zhu Y, Yang P. MicroRNA-16 suppresses epithelial-mesenchymal transition‐related gene expression in human glioma. Mol Med Rep 2014; 10(6):3310–4.

51. Yang T-Q, Lu X-J, Wu T-F, Ding D-D, Zhao Z-H, Chen G-L et al. MicroRNA-16 inhibits glioma cell growth and invasion through suppression of BCL2 and the nuclear factor-κB1/MMP9 signaling pathway. Cancer Sci 2014; 105(3):265–71.

52. Zhan X-H, Xu Q-Y, Tian R, Yan H, Zhang M, Wu J et al. MicroRNA16 regulates glioma cell proliferation, apoptosis and invasion by targeting Wip1-ATM-p53 feedback loop. Oncotarget 2017; 8(33):54788–98.

53. Zhou Y, Liu Y, Hu C, Jiang Y. MicroRNA-16 inhibits the proliferation, migration and invasion of glioma cells by targeting Sal-like protein 4. Int J Mol Med 2016; 38(6):1768–76.

54. Zhu Y, Xia Y, Niu H, Chen Y. MiR-16 induced the suppression of cell apoptosis while promote proliferation in oesophageal squamous cell carcinoma. Cell Physiol Biochem 2014; 33(5):1340–8.

55. Wang F, Fu X-D, Zhou Y, Zhang Y. Down-regulation of the cyclin E1 oncogene expression by microRNA-16-1 induces cell cycle arrest in human cancer cells. BMB Rep 2009; 42(11):725–30.

56. Yu X, Zhang X, Dhakal IB, Beggs M, Kadlubar S, Luo D. Induction of cell proliferation and survival genes by estradiol-repressed microRNAs in breast cancer cells. BMC Cancer 2012; 12:29.

57. Cornago M, Garcia-Alberich C, Blasco-Angulo N, Vall-Llaura N, Nager M, Herreros J et al. Histone deacetylase inhibitors promote glioma cell death by G2 checkpoint abrogation leading to mitotic catastrophe. Cell Death Dis 2014; 5:e1435.

58. Mir SE, De Witt Hamer, Philip C, Krawczyk PM, Balaj L, Claes A, Niers JM et al. In silico analysis of kinase expression identifies WEE1 as a gatekeeper against mitotic catastrophe in glioblastoma. Cancer Cell 2010; 18(3):244–57.

59. Sørensen CS, Syljuåsen RG. Safeguarding genome integrity: the checkpoint kinases ATR, CHK1 and WEE1 restrain CDK activity during normal DNA replication. Nucleic Acids Res 2012; 40(2):477–86.

60. Liu J, Chen G, Feng L, Zhang W, Pelicano H, Wang F et al. Loss of p53 and altered miR15-a/16-1□MCL-1 pathway in CLL: insights from TCL1-Tg:p53(-/-) mouse model and primary human leukaemia cells. Leukemia 2014; 28(1):118–28.

61. Gratas C, Séry Q, Rabé M, Oliver L, Vallette FM. Bak and Mcl-1 are essential for Temozolomide induced cell death in human glioma. Oncotarget 2014; 5(9):2428–35.

62. Murphy ÁC, Weyhenmeyer B, Noonan J, Kilbride SM, Schimansky S, Loh KP et al. Modulation of Mcl-1 sensitizes glioblastoma to TRAIL-induced apoptosis. Apoptosis 2014; 19(4):629–42.

63. Roth W, Grimmel C, Rieger L, Strik H, Takayama S, Krajewski S et al. Bag-1 and Bcl-2 gene transfer in malignant glioma: modulation of cell cycle regulation and apoptosis. Brain Pathol 2000; 10(2):223–34.

64. Strik H, Deininger M, Streffer J, Grote E, Wickboldt J, Dichgans J et al. BCL-2 family protein expression in initial and recurrent glioblastomas: modulation by radiochemotherapy. J Neurol Neurosurg Psychiatry 1999; 67(6):763–8.

65. Weller M, Malipiero U, Aguzzi A, Reed JC, Fontana A. Protooncogene bcl-2 gene transfer abrogates Fas/APO-1 antibody-mediated apoptosis of human malignant glioma cells and confers resistance to chemotherapeutic drugs and therapeutic irradiation. J Clin Invest 1995; 95(6):2633–43.

66. Xu J, Liao X, Wong C. Downregulations of B-cell lymphoma 2 and myeloid cell leukaemia sequence 1 by microRNA 153 induce apoptosis in a glioblastoma cell line DBTRG-05MG. Int J Cancer 2010; 126(4):1029–35.

67. Bellail AC, Olson JJ, Hao C. SUMO1 modification stabilizes CDK6 protein and drives the cell cycle and glioblastoma progression. Nat Commun 2014; 5:4234.

68. Yamashita Y, Kasugai I, Sato M, Tanuma N, Sato I, Nomura M et al. CDC25A mRNA levels significantly correlate with Ki-67 expression in human glioma samples. J Neurooncol 2010; 100(1):43–9.

69. Costello JF, Plass C, Arap W, Chapman VM, Held WA, Berger MS et al. Cyclin-dependent kinase 6 (CDK6) amplification in human gliomas identified using two-dimensional separation of genomic DNA. Cancer Res 1997; 57(7):1250–4.

70. Lam PY, Di Tomaso E, Ng HK, Pang JC, Roussel MF, Hjelm NM. Expression of p19INK4d, CDK4, CDK6 in glioblastoma multiforme. Br J Neurosurg 2000; 14(1):28–32.

71. Krajewski S, Krajewska M, Ehrmann J, Sikorska M, Lach B, Chatten J et al. Immunohistochemical analysis of Bcl-2, Bcl-X, Mcl-1, and Bax in tumours of central and peripheral nervous system origin. Am J Pathol 1997; 150(3):805–14.

72. Seol HJ, Yoo HY, Jin J, Joo KM, Kong D-S, Yoon SJ et al. Prognostic implications of the DNA damage response pathway in glioblastoma. Oncol Rep 2011; 26(2):423–30.

73. The Cancer Genome Atlas Research Network. Comprehensive genomic characterization defines human glioblastoma genes and core pathways. Nature 2008; 455(7216):1061–8.

74. Hirose Y, Berger MS, Pieper RO. Abrogation of the Chk1-mediated G(2) checkpoint pathway potentiates temozolomide-induced toxicity in a p53-independent manner in human glioblastoma cells. Cancer Res 2001; 61(15):5843–9.

75. Kwon J-E, Kim B-Y, Kwak S-Y, Bae I-H, Han Y-H. Ionizing radiation-inducible microRNA miR-193a-3p induces apoptosis by directly targeting Mcl-1. Apoptosis 2013; 18(7):896–909.

76. Li B, He H, Tao B-B, Zhao Z-Y, Hu G-H, Luo C et al. Knockdown of CDK6 enhances glioma sensitivity to chemotherapy. Oncol Rep 2012; 28(3):909–14.

77. Li R-Y, Chen L-C, Zhang H-Y, Du W-Z, Feng Y, Wang H-B et al. MiR-139 inhibits Mcl-1 expression and potentiates TMZ-induced apoptosis in glioma. CNS Neurosci Ther 2013; 19(7):477–83.

78. Han J, Chen Q. MiR-16 modulate temozolomide resistance by regulating BCL-2 in human glioma cells. Int J Clin Exp Pathol 2015; 8(10):12698–707.

79. Hui W, Yuntao L, Lun L, WenSheng L, ChaoFeng L, HaiYong H et al. MicroRNA-195 inhibits the proliferation of human glioma cells by directly targeting cyclin D1 and cyclin E1. PLoS ONE 2013; 8(1):e54932.

80. Ujifuku K, Mitsutake N, Takakura S, Matsuse M, Saenko V, Suzuki K et al. miR-195, miR-455-3p and miR-10a(*) are implicated in acquired temozolomide resistance in glioblastoma multiforme cells. Cancer Lett 2010; 296(2):241–8.

81. Patel N, Garikapati KR, Pandita RK, Singh DK, Pandita TK, Bhadra U et al. miR-15a/miR-16 down-regulates BMI1, impacting Ub-H2A mediated DNA repair and breast cancer cell sensitivity to doxorubicin. Sci Rep 2017; 7(1):4263.

82. Xia L, Zhang D, Du R, Pan Y, Zhao L, Sun S et al. miR-15b and miR-16 modulate multidrug resistance by targeting BCL2 in human gastric cancer cells. Int J Cancer 2008; 123(2):372–9.

83. Takeshita F, Patrawala L, Osaki M, Takahashi R-u, Yamamoto Y, Kosaka N et al. Systemic delivery of synthetic microRNA-16 inhibits the growth of metastatic prostate tumours via downregulation of multiple cell-cycle genes. Mol Ther 2010; 18(1):181–7.

84. van Zandwijk N, Pavlakis N, Kao SC, Linton A, Boyer MJ, Clarke S et al. Safety and activity of microRNA-loaded minicells in patients with recurrent malignant pleural

mesothelioma: a first-in-man, phase 1, open-label, dose-escalation study. Lancet Oncol 2017; 18(10):1386–96.

85. Kawano M, Tanaka K, Itonaga I, Iwasaki T, Tsumura H. c-Myc Represses Tumor-Suppressive microRNAs, let-7a, miR-16 and miR-29b, and Induces Cyclin D2-Mediated Cell Proliferation in Ewing's Sarcoma Cell Line. PLoS ONE 2015; 10(9):e0138560.

Acknowledgements

This study was supported by a grant from the Wilhelm Sander Foundation to MiWe, CH and GR (grant no. 2012.088.1) and a start-up grant from the Research Commission of the Medical Faculty of Heinrich Heine University to B.M. (grant no. 45/2010). We thank Professor V. Peter Collins, Cambridge, UK, for kindly providing the TP365MG glioma cell line. Parts of the reported results are based on data generated by the TCGA Research Network (http://cancergenome.nih.gov/).

Author Contributions

AK, MaWo, BM and GR designed the study protocol. AK and FL performed experiments based on primary glioma tissue samples and glioma cell cultures, and evaluated the data with the help of MaWo, BM and GR. MZ performed the biostatistical evaluations of the miRNA expression data. NS, CH and MiWe investigated the effect of irradiation and temozolomide on glioma cell lines following *miR-16-5p* overexpression. BM performed the TCGA data analyses. AK, MaWo, BM, CH and GR designed the figures. AK and GR wrote the manuscript with contributions and final approval by all authors.

Conflicts of interest

MiWe has received research grants from Abbvie, Acceleron, Actelion, Bayer, Merck, Sharp & Dohme (MSD), Merck (EMD), Novocure, OGD2, Piqur, Roche and Tragara, and honoraria for lectures or advisory board participation or consulting from Abbvie, BMS, Celgene, Celldex, Merck, Sharp & Dohme (MSD), Merck (EMD), Novocure, Orbus, Pfizer, Progenics, Roche, Teva and Tocagen. GR has received research grants from Roche and Merck, and

honoraria for advisory boards from Abbvie. The other authors declare no conflict of interest. The Editors of Neuropathology and Applied Neurobiology are committed to peer review integrity and upholding the highest standards of review. As such, this article was peer reviewed by independent, anonymous expert referees and the corresponding author (GR) had no role in either the editorial decision or the handling of the paper.

Supplementary material

Supplementary material is available online at the journal's homepage.

Legends to the figures

Figure 1. ***Expression of miR-16-5p in gliomas and glioma cell lines.*** **(A, B)** *MiR-16-5p* expression profiling using TaqMan® Array MicroRNA Cards in 9 non-neoplastic brain tissue (NB) and 79 gliomas including 7 diffuse astrocytomas, IDH-mutant, WHO grade II (AII^{mut}), 10 anaplastic astrocytomas, IDH-mutant, WHO grade III ($AAIII^{mut}$), 10 glioblastomas, IDH-mutant, WHO grade IV ($GBIV^{mut}$), and 52 glioblastomas, IDH-wildtype, WHO grade IV ($GBIV^{wt}$). Box plots indicate normalized median expression values as well as lower and upper quartiles. Whiskers indicate lowest and highest expression levels. **(A)** Glioma groups were compared to the NB group by ANOVA and Dunnett's post hoc test. **(B)** 52 IDH-wildtype were compared to 27 IDH-mutant gliomas using two-sided unpaired Student´s t-test **(C)** *MiR-16-5p* expression as determined by targeted realtime RT-PCR. Six glioma cell lines (A172, T98G, TP365MG, U138MG, U87MG, U251MG, abbreviated as CL) were compared to ten non-neoplastic brain tissue samples (NB) using two-sided unpaired Student´s t-test. In all graphs, asterisks indicate significant expression differences (*, $p < 0.05$; **, $p < 0.01$; ****, $p < 0.0001$).

Figure 2. ***Decreased viability and proliferation as well as increased caspase-3/7 activity following overexpression of miR-16-5p in glioma cells.*** Glioma cells were transiently transfected with 25 nM (viability and proliferation) or 50 nM (caspase-3/7 activity) pre-miR-16-5p or pre-miR-NC controls for 72 hours. Graphs depict cell viability **(A)**, proliferation **(B)** and caspase-3/7 activity **(C)** for the cell lines A172, TP98G, and TP365MG. Dots represent the mean of 5 replicate measurements. Three independent experiments were performed per cell line. P-values are calculated using a mixed model. For calculations, the fixed variable was the transfection group and the random variable was the week of transfection. RLU, relative luminescence units; RFU, relative fluorescence units.

Figure 3. ***MRNA expression and protein levels of selected miR-16-5p target genes following transfection of miR-16-5p precursors in A172 glioma cells.*** **(A)** Shown are results of realtime-RT-PCR expression analyses using *ARF1* as reference transcript. Three independent experiments were performed. P-values refer to two-sided paired Student´s t-tests. Note reduced expression of *CDK6, CCND3, CCNE1, CDC25A, WEE1,* and *CHEK1* but not *BCL2* and *MCL1* transcripts after *miR-16-5p* overexpression. Exemplary results of Western blot analyses **(B)** and its quantifications **(C)** in A172 glioma cells transiently transfected with pre-miR-16-5p or pre-miR-NC are shown. Blots were immunostained for ß-actin (ACTB) to normalize the protein levels in the individual lanes. Note that all eight target proteins, including BCL2 and MCL1, were down-regulated by *miR-16-5p* overexpression relative to control transfected cells **(B, C)**.

Figure 4. ***Demonstration of direct binding of miR-16-5p to the 3'-UTRs of WEE1, CHEK1, and MCL1 using luciferase reporter assay.*** **(A)** Schematic representation of *miR-16-5p* binding sites in the 3'-UTR of the target genes *WEE1, CHEK1*, *MCL1* that were cloned into psiCHECK-2™ plasmids with flanking nucleotides. Bold bases represent bases comprising the recognition sites for the miRNA seed sequence that were mutated (mut, mut1, mut2, mut1,2) to ensure specific miRNA binding. **(B)** T98G glioma cells were transiently co-transfected with either 100 ng *WEE1*, *CHEK1 or MCL1* wildtype (wt) or mutated 3´-UTR reporter constructs and 50 nM pre-miR-16-5p or pre-miR-NC for 72 hours (*WEE1*) or 48 hours (*CHEK1* and *MCL1*). Bars and error bars represent the mean results of three independent experiments and standard errors of the mean. Each experiment comprised 5 replicates. P-values refer to two-sided, paired Student´s t-tests (*, $p < 0.05$; ***, $p < 0.001$). RLU, relative luminescence units.

Figure 5. MRNA expression of several *miR-16-5p* target genes in gliomas. Results of microarray expression analyses of four non-neoplastic brain tissue (NB) and 68 human gliomas, including 8 AII^{mut}, 10 $AAIII^{mut}$, 11 $GBIV^{mut}$, and 39 $GBIV^{wt}$ are shown. Box plots are

depicted indicating median expression as well as lower and upper quartiles. Whiskers indicate lowest and highest expression values. Comparison between each tumour group and the non-neoplastic brain tissue group (NB) was performed by ANOVA and Dunnett's post hoc test. Asterisks indicate significant expression differences (*, $p < 0.05$; **, $p < 0.01$; ***, $p < 0.001$).

Figure 6. ***Treatment with trichostatin A (TSA) as well as siRNA-mediated HDAC3 knockdown increases miR-16-5p expression in glioma cells.*** **(A)** Glioma cells were treated with 1 µM TSA for 36 hours. Shown are real-time RT-PCR results for *miR-16-5p* in A172, T98G, TP365MG, and U138MG cells. Each dot represents data from two technical replicates. Three independent experiments were performed. **(B-D)** Results of *HDAC3* knockdown in T98G and U251MG glioma cells. Transfection of two siRNAs against *HDAC3* (si_HDAC3-1, si_HDAC3-2) effectively reduced *HDAC3* at the mRNA **(B)** and protein level **(C)** as compared to control transfected cells (si_NC). *ARF1* was used to normalize mRNA expression and ACTB to normalize protein expression. *HDAC3* knockdown resulted in significantly increased expression (black squares) of *miR-16-5p* as well as significantly reduced expression (white squares) of most of the investigated *miR-16-5p* target genes. Three independent transfections were performed. P-values were calculated using the two-sided, paired Student´s t-test (*, $p < 0.05$; ** $p < 0.01$).

Figure 7. ***Modulation of glioma cell sensitivity to irradiation and temozolomide treatment by transfection of miR-16-5p precursors.*** Pre-miR-16-5p-transfected (black squares) or pre-miR-NC control-transfected (open circles) A172 cells (A, C) or T98G cells (B, D) were exposed to increasing concentrations of TMZ for 24 h (A, B) or irradiated at increasing doses (C, D) and allowed to grow for 2-3 weeks in complete medium. Cell density was assessed by crystal violet staining. Data were assessed in triplets. Shown are diagrams of one of three independent replica experiments each (*, $p < 0.05$; **, $p < 0.01$; ***, $p < 0.001$, two-sided student's T-test).

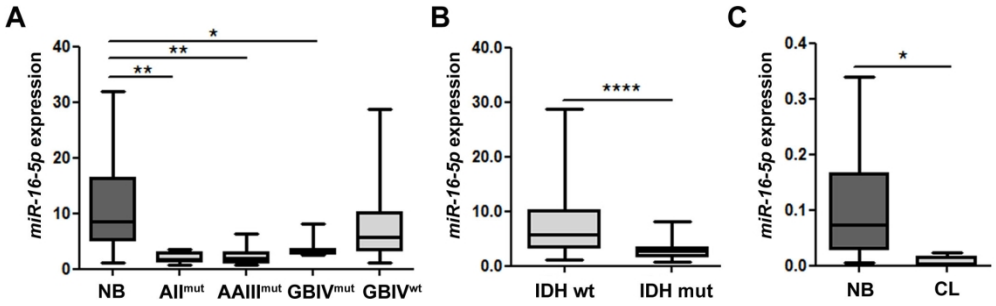

Figure 1. Expression of miR-16-5p in gliomas and glioma cell lines. (A, B) MiR-16-5p expression profiling using TaqMan® Array MicroRNA Cards in 9 non-neoplastic brain tissue (NB) and 79 gliomas including 7 diffuse astrocytomas, IDH-mutant, WHO grade II (AIImut), 10 anaplastic astrocytomas, IDH-mutant, WHO grade III (AAIIImut), 10 glioblastomas, IDH-mutant, WHO grade IV (GBIVmut), and 52 glioblastomas, IDH-wildtype, WHO grade IV (GBIVwt). Box plots indicate normalized median expression values as well as lower and upper quartiles. Whiskers indicate lowest and highest expression levels. (A) Glioma groups were compared to the NB group by ANOVA and Dunnett's post hoc test. (B) 52 IDH-wildtype were compared to 27 IDH-mutant gliomas using two-sided unpaired Student´s t-test (C) MiR-16-5p expression as determined by targeted realtime RT-PCR. Six glioma cell lines (A172, T98G, TP365MG, U138MG, U87MG, U251MG, abbreviated as CL) were compared to ten non-neoplastic brain tissue samples (NB) using two-sided unpaired Student´s t-test. In all graphs, asterisks indicate significant expression differences (*, $p < 0.05$; **, $p < 0.01$; ****, $p < 0.0001$).

180x58mm (300 x 300 DPI)

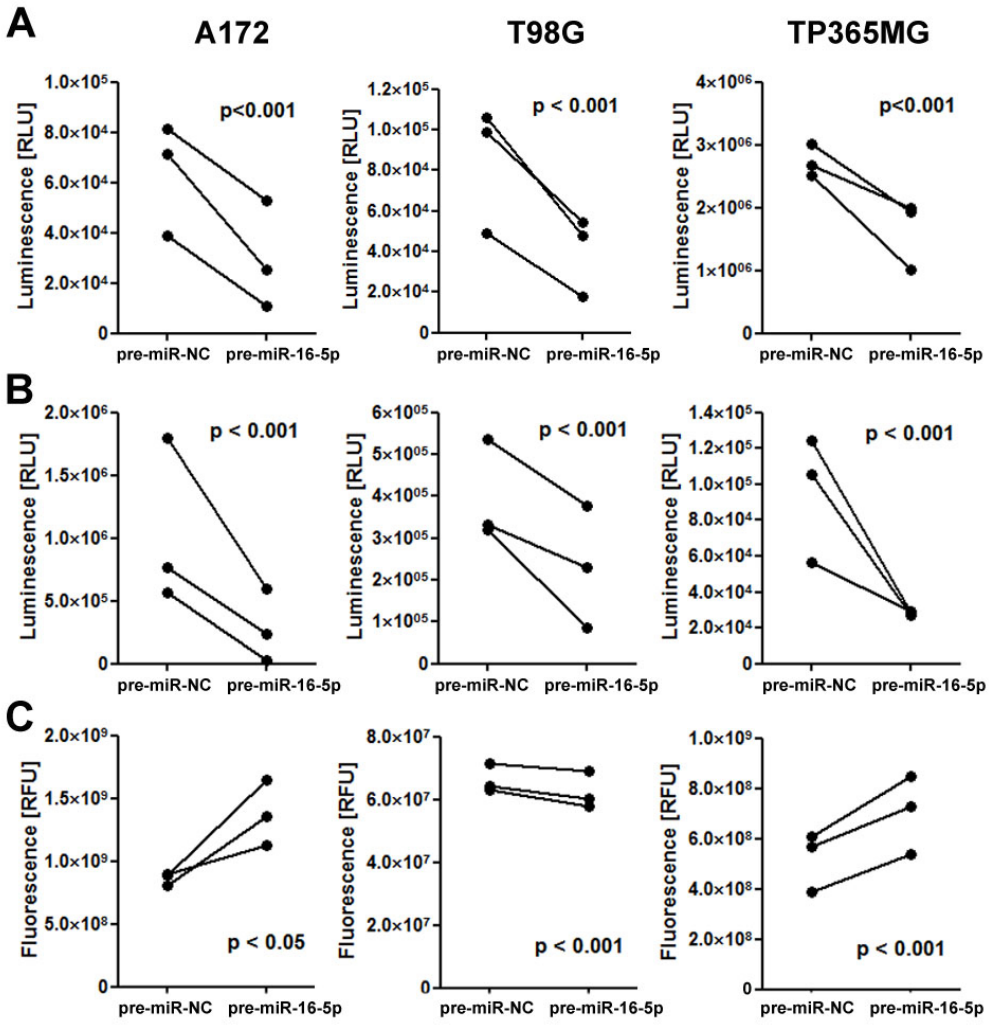

Figure 2. Decreased viability and proliferation as well as increased caspase-3/7 activity following overexpression of miR-16-5p in glioma cells. Glioma cells were transiently transfected with 25 nM (viability and proliferation) or 50 nM (caspase-3/7 activity) pre miR 16-5p or pre-miR-NC controls for 72 hours. Graphs depict cell viability (A), proliferation (B) and caspase-3/7 activity (C) for the cell lines A172, TP98G, and TP365MG. Dots represent the mean of 5 replicate measurements. Three independent experiments were performed per cell line. P-values are calculated using a mixed model. For calculations, the fixed variable was the transfection group and the random variable was the week of transfection. RLU, relative luminescence units; RFU, relative fluorescence units

80x83mm (300 x 300 DPI)

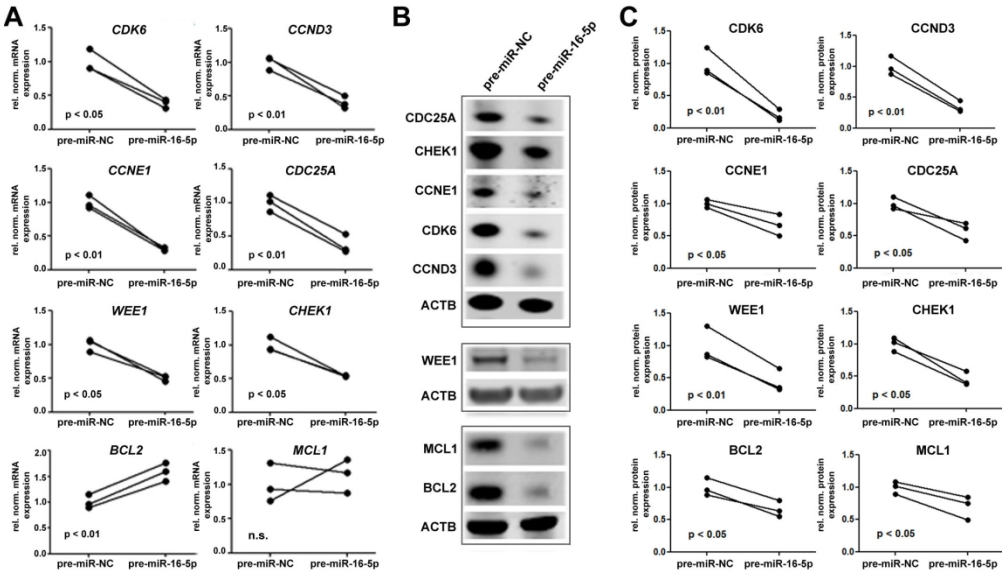

Figure 3. MRNA expression and protein levels of selected miR-16-5p target genes following transfection of miR-16-5p precursors in A172 glioma cells. (A) Shown are results of realtime-RT-PCR expression analyses using ARF1 as reference transcript. Three independent experiments were performed. P-values refer to two-sided paired Student´s t-tests. Note reduced expression of CDK6, CCND3, CCNE1, CDC25A, WEE1, and CHEK1 but not BCL2 and MCL1 transcripts after miR-16-5p overexpression. Exemplary results of Western blot analyses (B) and its quantifications (C) in A172 glioma cells transiently transfected with pre-miR-16-5p or pre-miR-NC are shown. Blots were immunostained for ß-actin (ACTB) to normalize the protein levels in the individual lanes. Note that all eight target proteins, including BCL2 and MCL1, were down-regulated by miR-16-5p overexpression relative to control transfected cells (B, C).

180x109mm (300 x 300 DPI)

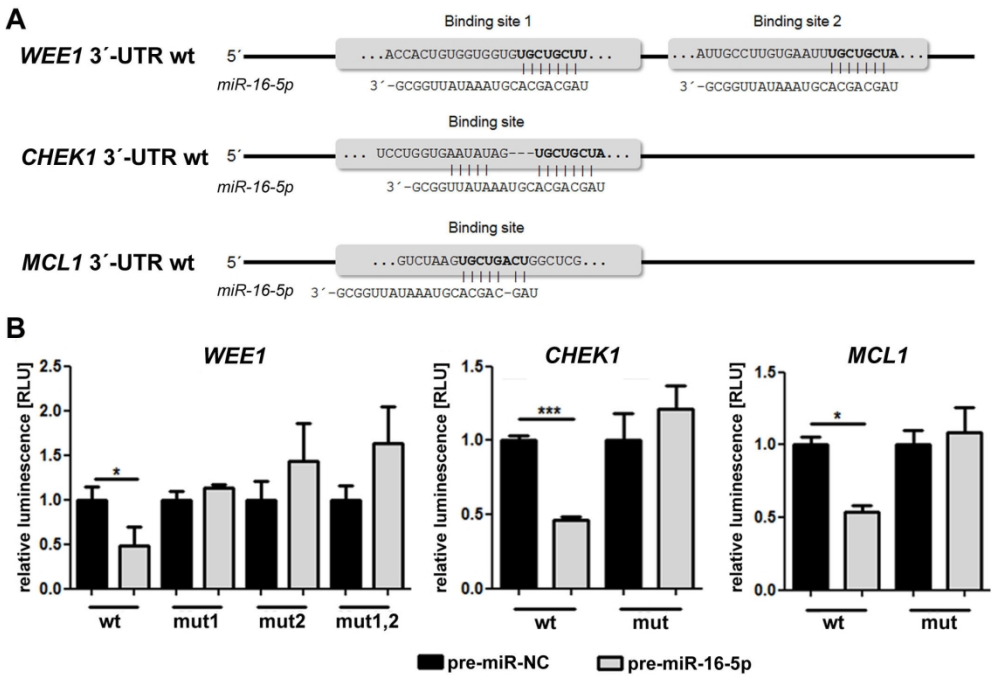

Figure 4. Demonstration of direct binding of miR-16-5p to the 3'-UTRs of WEE1, CHEK1, and MCL1 using luciferase reporter assay. (A) Schematic representation of miR 16 5p binding sites in the 3'-UTR of the target genes WEE1, CHEK1, MCL1 that were cloned into psiCHECK-2TM plasmids with flanking nucleotides. Bold bases represent bases comprising the recognition sites for the miRNA seed sequence that were mutated (mut, mut1, mut2, mut1,2) to ensure specific miRNA binding. (B) T98G glioma cells were transiently co-transfected with either 100 ng WEE1, CHEK1 or MCL1 wildtype (wt) or mutated 3´-UTR reporter constructs and 50 nM pre-miR-16-5p or pre-miR-NC for 72 hours (WEE1) or 48 hours (CHEK1 and MCL1). Bars and error bars represent the mean results of three independent experiments and standard errors of the mean. Each experiment comprised 5 replicates. P-values refer to two-sided, paired Student´s t-tests (*, $p < 0.05$; ***, $p < 0.001$). RLU, relative luminescence units.

180x123mm (300 x 300 DPI)

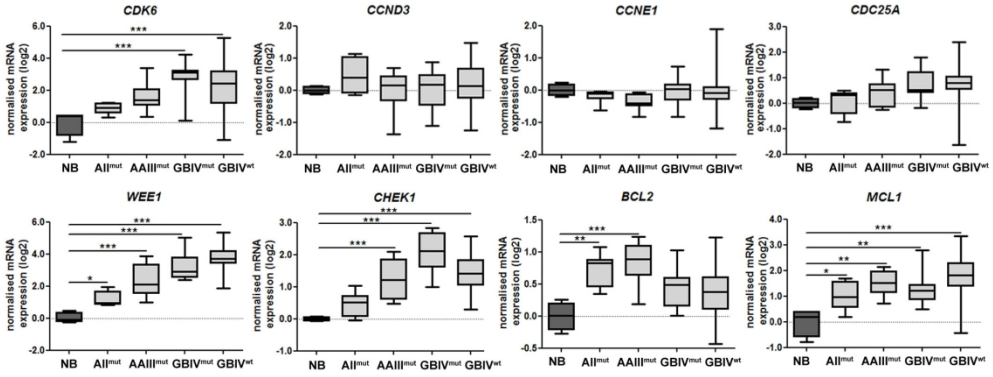

Figure 5. MRNA expression of several miR-16-5p target genes in gliomas. Results of microarray expression analyses of four non-neoplastic brain tissue (NB) and 68 human gliomas, including 8 AIImut, 10 AAIIImut, 11 GBIVmut, and 39 GBIVwt are shown. Box plots are depicted indicating median expression as well as lower and upper quartiles. Whiskers indicate lowest and highest expression values. Comparison between each tumour group and the non-neoplastic brain tissue group (NB) was performed by ANOVA and Dunnett's post hoc test. Asterisks indicate significant expression differences (*, $p < 0.05$; **, $p < 0.01$; ***, $p < 0.001$).

180x72mm (300 x 300 DPI)

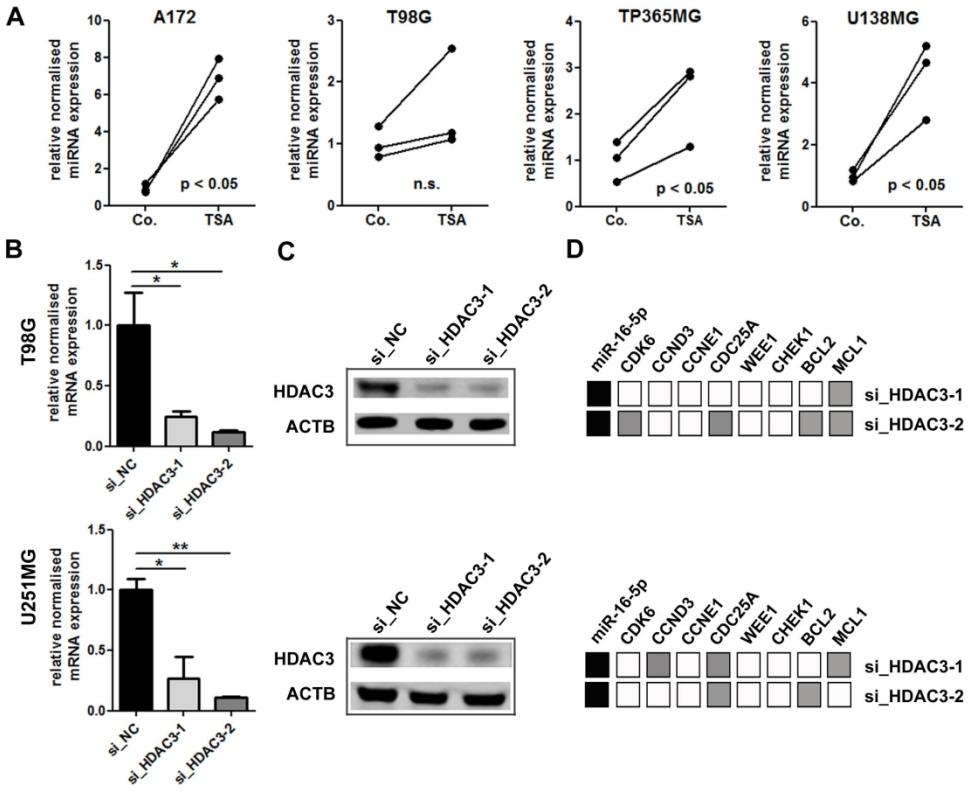

Figure 6. Treatment with trichostatin A (TSA) as well as siRNA-mediated HDAC3 knockdown increases miR-16-5p expression in glioma cells. (A) Glioma cells were treated with 1 µM TSA for 36 hours. Shown are real-time RT-PCR results for miR-16-5p in A172, T98G, TP365MG, and U138MG cells. Each dot represents data from two technical replicates. Three independent experiments were performed. (B-D) Results of HDAC3 knockdown in T98G and U251MG glioma cells. Transfection of two siRNAs against HDAC3 (si_HDAC3-1, si_HDAC3-2) effectively reduced HDAC3 at the mRNA (B) and protein level (C) as compared to control transfected cells (si_NC). ARF1 was used to normalize mRNA expression and ACTB to normalize protein expression. HDAC3 knockdown resulted in significantly increased expression (black squares) of miR-16-5p as well as significantly reduced expression (white squares) of most of the investigated miR-16-5p target genes. Three independent transfections were performed. P-values were calculated using the two-sided, paired Student´s t-test (*, $p < 0.05$; ** $p < 0.01$).

180x145mm (300 x 300 DPI)

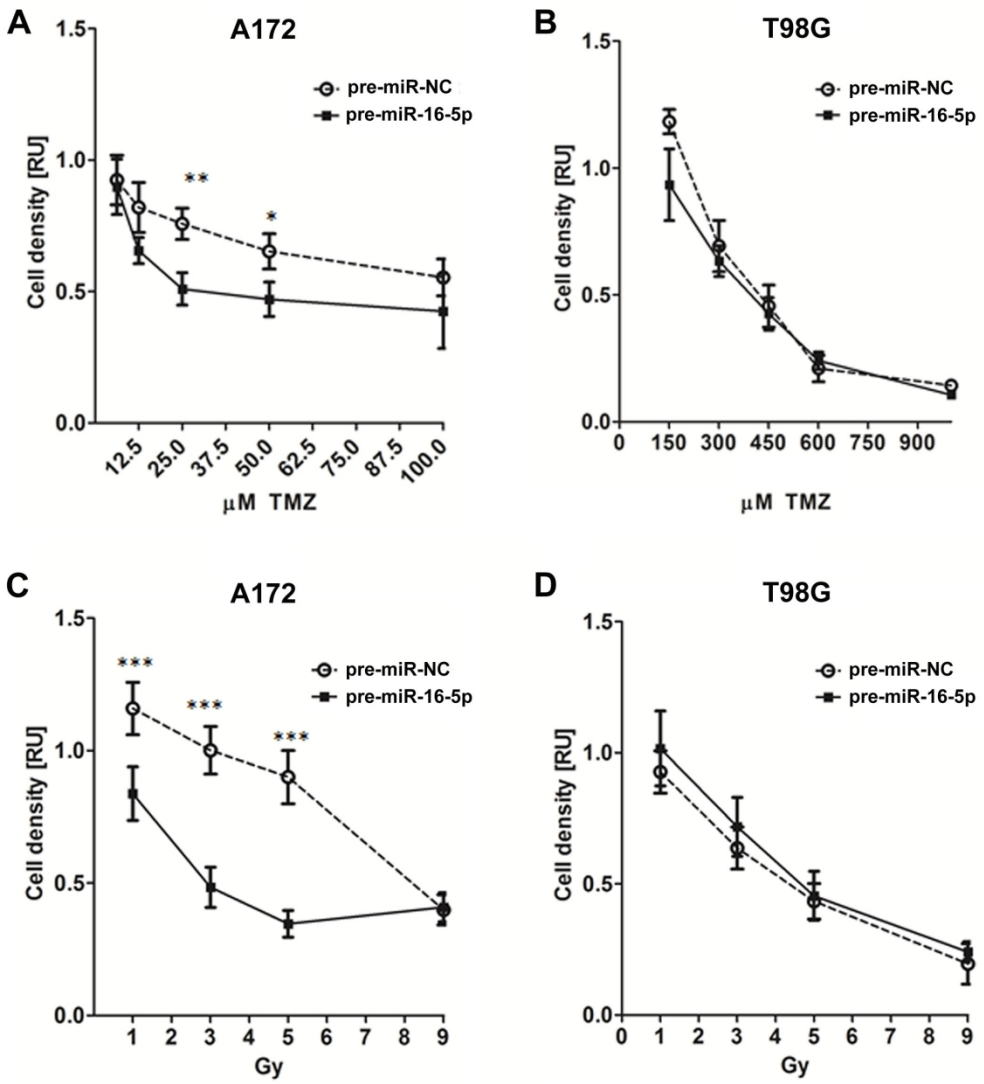

Figure 7. Modulation of glioma cell sensitivity to irradiation and temozolomide treatment by transfection of miR-16-5p precursors. Pre-miR-16-5p-transfected (black squares) or pre-miR-NC control-transfected (open circles) A172 cells (A, C) or T98G cells (B, D) were exposed to increasing concentrations of TMZ for 24 h (A, B) or irradiated at increasing doses (C, D) and allowed to grow for 2-3 weeks in complete medium. Cell density was assessed by crystal violet staining. Data were assessed in triplets. Shown are diagrams of one of three independent replica experiments each (*, $p < 0.05$; **, $p < 0.01$; ***, $p < 0.001$, two-sided student's T-test).

180x194mm (300 x 300 DPI)

MiR-16-5p is frequently down-regulated in astrocytic gliomas and modulates glioma cell proliferation, apoptosis, and response to cytotoxic therapy

Anneliese Krell,[1#] Marietta Wolter,[1#] Nina Stojcheva,[2] Caroline Hertler,[2] Franziska Liesenberg,[1] Marc Zapatka,[3] Michael Weller,[2] Bastian Malzkorn,[1*] Guido Reifenberger[1,4*]

[1]Department of Neuropathology, Heinrich Heine University, Düsseldorf, Germany; [2]Department of Neurology, University Hospital Zurich, Zurich, Switzerland; [3]Division of Molecular Genetics, German Cancer Research Center, Heidelberg, Germany; [4]German Cancer Consortium (DKTK), partner site Essen/Düsseldorf, DKFZ, Heidelberg, Germany

Supplementary material

Supplementary Table 1. Overview of primer sequences used for (1) qRT-PCR, (2, 3) luciferase reporter gene assay (2: with the wildtype binding sequence, and 3: with the mutated binding site for *miR-16-5p*).

Gene	Accession-No.	Chromosome	Primer sequence	Remarks	Amplicon length	Application
CDK6	NM_001259.6	7q21.2	5´-TGCACAGTGTCACGAACAGA 5´-ACCTCGGAGAAGCTGAAACA	forward reverse	150 bp	1
CCND3	NM_001136017.3	6p21.1	5´-CATGCCCAGACCTTTTTGGC 5´-CAGTCCACTTCAGTGCCAGT	forward reverse	176 bp	1
CCNE1	NM_001238.2	19q12	5´-CAGATTGCAGAGCTGTTGGA 5´-TCCCCGTCTCCCTTATAACC	forward reverse	199 bp	1
CDC25A	NM_001789.2	3p21.31	5´-TGGCAAGCGTGTCATTGTTG 5´-AGCTAGGGGGCTCACAGTAA	forward reverse	194 bp	1
WEE1	NM_001143976	11p15.4	5´-GAGTACTGCGCAGATGACCA 5´-GAGGAGTCTGTCGCACATCA	forward reverse	230 bp	1
			5´-gggtatctcgagGACAAGAGGAAGCTAGGTTG 5´-ggctatgcggccgcAACACAAGTCAAAGACAAGTGC	forward reverse	1075 bp	2
CHEK1	NM_001114122.2	11q24.2	5´-TTACTGCAATGCTCGCTGGA 5´-TGGGAGACTCTGACACACCA	forward reverse	270 bp	1
			5´-gggtatctcgagCTGGGGAATCCTGGTGAATAT 5´-ggctatgcggccgcGTTTTGAAGCTGGCTTCGCT	forward reverse	461 bp	2
			5´-gggtatctcgagCTGGGGAATCCTGGTGAATATAGGTAG TAGCTGTTGAC 5´-ggctatgcggccgcGTTTTGAAGCTGGCTTCGCT	forward reverse	461 bp	3
BCL-2	NM_001127240.2	19q13.32	5´-GAGGATTGTGGCCTTCTTTG 5´-ACAGTTCCACAAAGGCATCCCA	forward reverse	170 bp	1
MCL-1	NM_021960.4	1q21.3	5´-TCTCTCGGTACCTTCGGGAG 5´-AACCCATCCCAGCCTCTTTG	forward reverse	400 bp	1
HDAC3	NM_003883.3	5q31.3	5´-GGAGCTGGACACCCTATGAA 5´-GACTCTTGGTGAAGCCTTGC	forward reverse	199 bp	1
DLEU2	NR_002612.1	13q14.2	5´-GAGGGCAATAAATGCCACAT 5´-GTGGTCCAGAAAACCTGCTC	forward reverse	109 bp	1
ARF1	NM_001658.3	1q42.13	5´-GACCACGATCCTCTACAAGC 5´-TCCCACACAGTGAAGCTGATG	forward reverse	111 bp	1
B2M	NM_004048.2	15q21.1	5´-GTTGCTCCACAGGTAGCTCTAG 5´-ACAAGCTTTGAGTGCAAGAGATTG	forward reverse	123 bp	4
			5´-GTCTCGCTCCGTGGCCTTAG 5´-CATTCTCTGCTGGATGACGTGAG	forward reverse	110 bp	4
psiCHECK2	plasmid		5´-AGGACGCTCCAGATGAAAT 5´-CAAACCCTAACCACCGCT	forward reverse	*	5

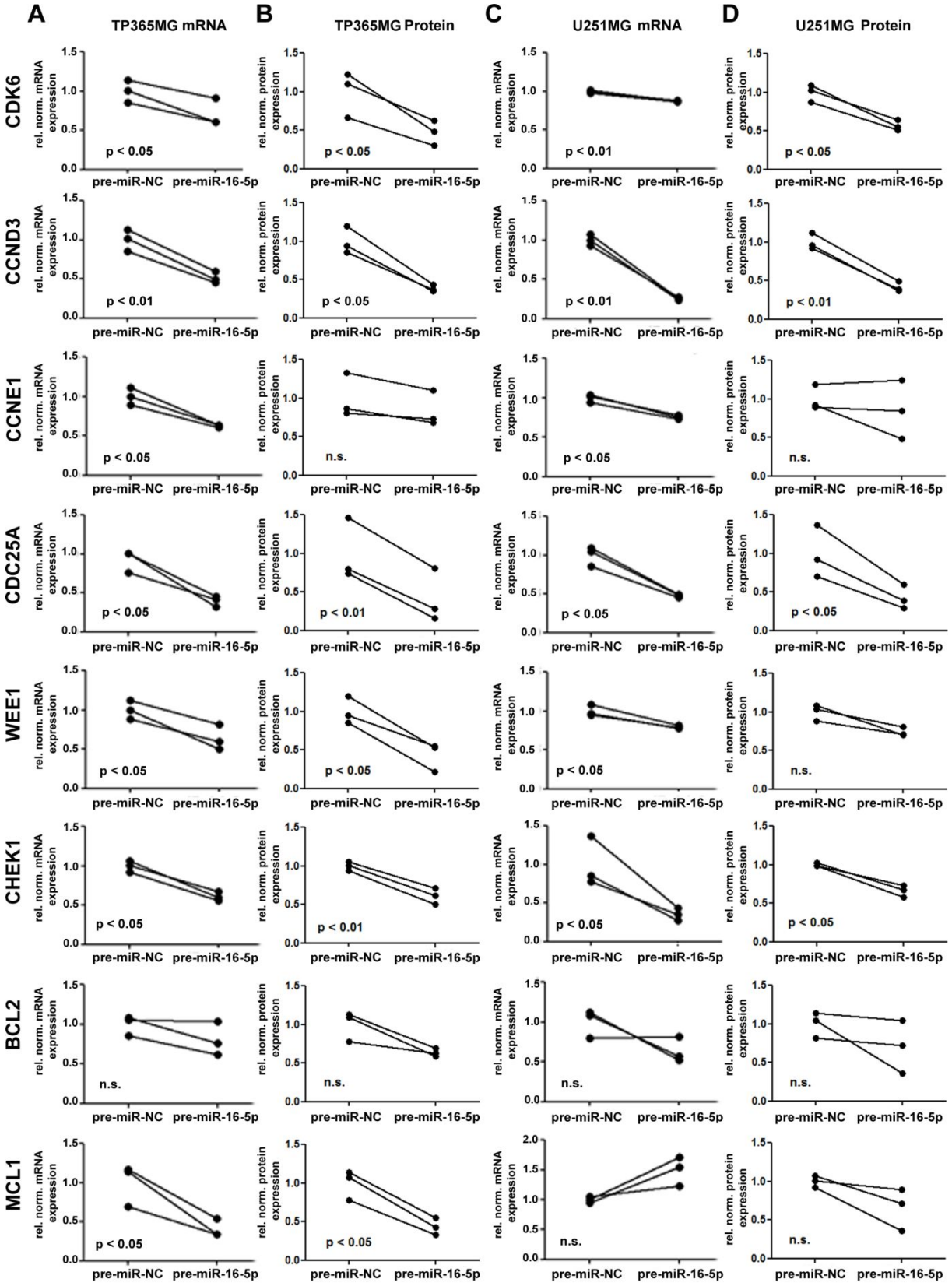

Supplementary Figure 1. ***Decreased expression of selected target genes following transfection of miR-16-5p precursors in TP365MG and U251MG glioma cells.*** **(A, C)** Results

of qRT-PCR expression analyses using *ARF1* as reference. Three independent experiments were performed. P-values refer to two-sided paired Student´s t-tests. **(B, D)** Quantification of Western blot analyses. Blots were immunostained for beta-actin (ACTB) to normalize protein levels in the individual lanes.

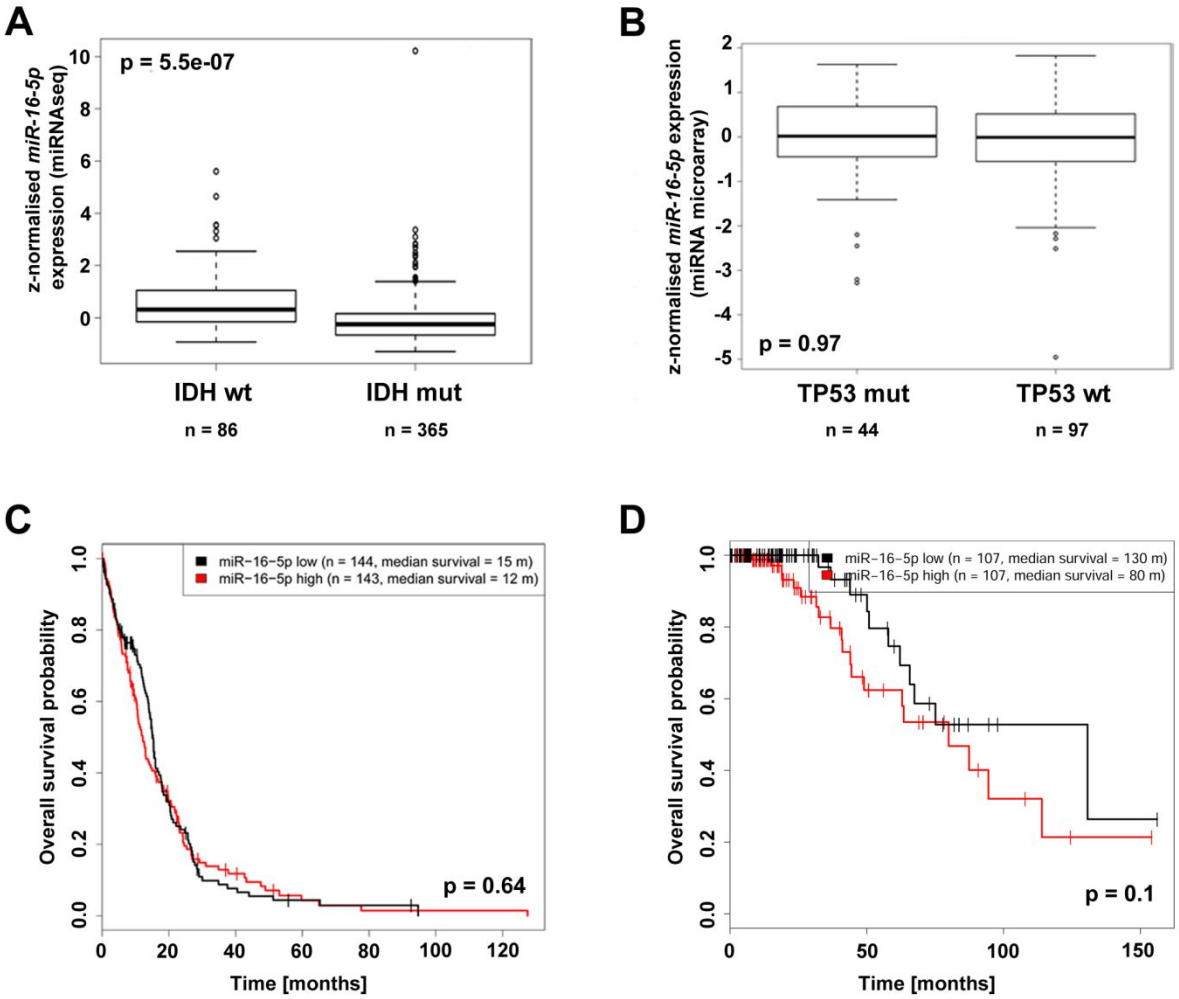

Supplementary Figure 2. ***Results based on correlative analyses of TCGA data sets,*** **(A)** Lower expression of *miR-16-5p* in IDH-mutant (IDH mut, n=365) as compared to IDH-wildtype gliomas from the TCGA-LGG dataset (IDH wt, n= 86). **(B)** *MiR-16-5p* expression does not differ between *TP53*-wildtype and *TP53*-mutant IDH-wildtype glioblastomas (n=141). **(C-D)** *MiR-16-5p* expression is not linked to overall survival in IDH-wildtype glioblastoma patients (n = 287) **(C)** and in IDH-mutant diffuse and anaplastic astrocytoma patients (n=214) **(D)**.

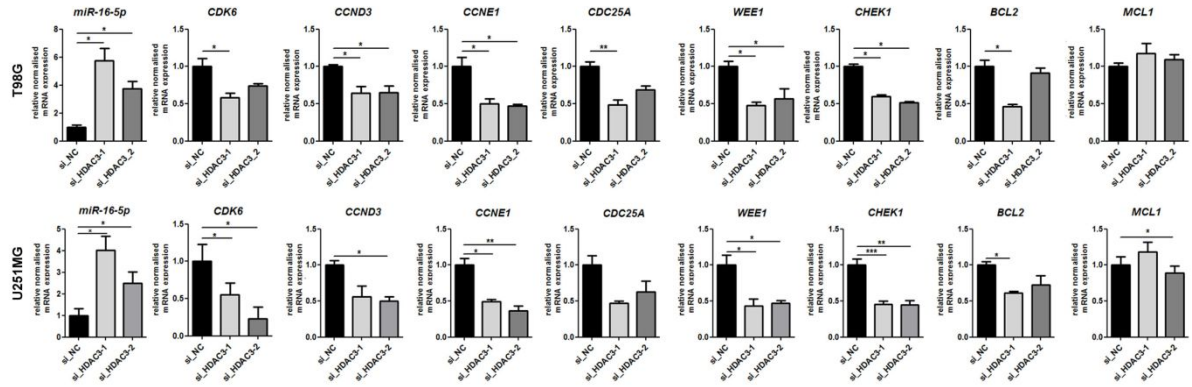

Supplementary Figure 3. ***Increased expression of miR-16-5p and reduced expression of its target genes in T98G and U251MG glioma cells following HDAC3 knock-down.*** Results of qRT-PCR using U6 snRNA as reference for miRNA expression analysis and *ARF1* as reference gene for mRNA expression analysis in T98G or U251MG cells transiently transfected with 50 nM siRNA against *HDAC3*. Three independent experiments were performed. P-values refer to two-sided paired Student´s t-tests.